Hunter-gatherer impact on European interglacial vegetation: a modelling approach

Nikulina, A.; MacDonald, K.; Zapolska, A.; Serge, M.A.; Roche, D.M.; Mazier, F.; ... ; Scherjon, F.

Quaternary Science Reviews 324 (2024) 108439

Contents lists available at ScienceDirect

Quaternary Science Reviews

journal homepage: www.elsevier.com/locate/quascirev

Hunter-gatherer impact on European interglacial vegetation: A modelling approach

Anastasia Nikulina [a,*], Katharine MacDonald [a,1], Anhelina Zapolska [b], Maria Antonia Serge [c], Didier M. Roche [b,d], Florence Mazier [c], Marco Davoli [e,f], Jens-Christian Svenning [e], Dave van Wees [b,g], Elena A. Pearce [e], Ralph Fyfe [h], Wil Roebroeks [a], Fulco Scherjon [a,i]

[a] Faculty of Archaeology, Department of World Archaeology, Human Origins Group, Leiden University, Einsteinweg 2, Leiden, 2333CC, the Netherlands
[b] Earth and Climate Cluster, Faculty of Sciences, Vrije Universiteit Amsterdam, De Boelelaan 1085, Amsterdam, 101 HV, the Netherlands
[c] Laboratoire Géographie de l'Environnement, UMR 5602, CNRS, Université de Toulouse-Jean Jaurès, Toulouse, 31058, France
[d] Laboratoire des Sciences du Climat et de l'Environnement, LSCE/IPSL, CEA-CNRS-UVSQ, Université Paris-Saclay, Gif-sur-Yvette, 91191, France
[e] Center for Ecological Dynamics in a Novel Biosphere (ECONOVO) & Center for Biodiversity Dynamics in a Changing World (BIOCHANGE), Department of Biology, Aarhus University, Ny Munkegade 114, Aarhus C, DK-8000, Denmark
[f] Department of Biology and Biotechnology "Charles Darwin", La Sapienza University, Viale dell'Universita' 32, 00185 Rome, Italy
[g] BeZero Carbon Ltd, Gorsuch Place, Senna Building, E2 8JF, London, UK
[h] School of Geography, Earth and Environmental Sciences, University of Plymouth, Plymouth, PL4 8AA, United Kingdom
[i] MONREPOS Archaeological Research Centre and Museum for Human Behavioural Evolution, Römisch-Germanisches Zentralmuseum, Schloss Monrepos, Neuwied, 56567, Germany

ARTICLE INFO

Handling Editor: Dr Donatella Magri

Keywords:
Agent-based modelling
Hunter-gatherers
Europe
Vegetation modelling
Landscape burning
HUMLAND

ABSTRACT

This article focuses on hunter-gatherer impact on interglacial vegetation in Europe, using a case study from the Early Holocene (9200–8700 BP). We present a novel agent-based model, hereafter referred to as HUMLAND (HUMan impact on LANDscapes), specifically developed to define key factors in continental-level vegetation changes via assessment of differences between pollen-based reconstruction and dynamic global vegetation model output (climate-based vegetation cover). The identified significant difference between these two datasets can be partially explained by the difference in the models themselves, but also by the fact that climate is not the sole factor responsible for vegetation change. Sensitivity analysis of HUMLAND showed that the intensity of anthropogenic vegetation modification mainly depended on three factors: the number of groups present, their preferences for vegetation openness around campsites, and the size of an area impacted by humans. Overall, both climate and human activities had strong impacts on vegetation openness during the study period. Our modelling results support the hypothesis that European ecosystems were strongly shaped by human activities already in the Mesolithic.

1. Introduction

The history of anthropogenic impacts on the environment spans over millennia, with humans already engaging in landscape transformations before the emergence of agriculture (Ellis et al., 2016, 2021; Nikulina et al., 2022; Zapolska et al., 2023a). Ethnographic observations show that hunter-gatherers or foragers (i.e., groups that mainly depend on food collection or foraging of wild resources) (Ember, 2020) influence their surroundings in several ways including modification of vegetation communities via burning (Rowley-Conwy and Layton, 2011; Smith, 2011; Scherjon et al., 2015; Nikulina et al., 2022). This practice was identified for all vegetation types except tundra at different spatial scales and for diverse objectives including driving game, stimulating the growth of edible plants, and clearing pathways (Scherjon et al., 2015).

Besides ethnographic data, evidence from archaeological contexts show that fire use was an important part of the technological repertoire of the *Homo* lineage since at least the second half of the Middle Pleistocene (e.g., Roebroeks and Villa, 2011; Gowlett and Wrangham, 2013; Sorensen et al., 2018). Human-induced vegetation burning during the Late Pleistocene has been proposed as a potential factor in several case

* Corresponding author.
E-mail addresses: a.nikulina@arch.leidenuniv.nl, nikulina1302@gmail.com (A. Nikulina).
[1] Deceased.

https://doi.org/10.1016/j.quascirev.2023.108439
Received 8 September 2023; Received in revised form 11 November 2023; Accepted 26 November 2023
Available online 21 December 2023

studies spanning various continents (Summerhayes et al., 2010; Pinter et al., 2011; Hunt et al., 2012; Thompson et al., 2021). Notably, the earliest evidence of a local-scale impact of fire use was identified at the Neumark-Nord site in Germany, dated to the Last Interglacial (Eemian, ~130,000–116,000 BP) (Roebroeks et al., 2021). In addition, fire-using foragers were suggested as one of the primary drivers of vegetation openness in Europe during the Last Glacial Maximum, i.e., possibly constituting one of the earliest large-scale anthropogenic modifications of Earth's systems (Kaplan et al., 2016).

While these Pleistocene cases are still subject to debate, hunter-gatherer-induced vegetation burning during the Early–Middle Holocene (~11,700–6000 BP) is generally accepted (Zvelebil, 1994; Mason, 2000; Davies et al., 2005; Dietze et al., 2018), even though the quality of the data is not necessarily that different from the earlier ones (Nikulina et al., 2022). However, the number of case studies is higher for the Early–Middle Holocene than for the Pleistocene. Most of the Early–Middle Holocene evidence comes from Europe (e.g., Caseldine and Hatton, 1993; Mellars and Dark, 1998; Bos and Urz, 2003; Gumiński and Michniewicz, 2003; Hörnberg et al., 2006; Woldring et al., 2012; Innes et al., 2013; Kaal et al., 2013; Hjelle and Lødøen, 2017; Milner et al., 2018; Heidgen et al., 2022; Sevink et al., 2023).

Despite the presence of case studies for anthropogenic burning (intentional or not) of past landscapes by hunter-gatherers, it is still difficult to establish whether these local-scale activities caused changes at regional and/or even (sub-)continental scales (Nikulina et al., 2022). Furthermore, overall landscape dynamics do not only depend on humans, and rather represent the complex interplay of natural and cultural processes at different spatio-temporal scales (Tasser et al., 2009). Landscapes are complex systems where heterogeneous components interact to impact on ecological processes, and might demonstrate non-linear dynamics and emergence (Newman et al., 2019). Therefore, it is often challenging to identify specific types of impacts on landscapes using proxy-based reconstructions (e.g., palynological datasets).

Modelling approaches offer excellent opportunities to explore how complex system components might interact, particularly when real-time experiments are not possible. Spatially explicit agent-based modelling (ABM) is commonly used to explore complex systems where multiple factors intertwine, and to propose possible scenarios of system functioning (Romanowska et al., 2021). Importantly, the outcomes of ABM exercises can be compared to empirical data. The ABM approach has been applied in various contexts to study past human-environment interactions and land use/land cover changes, such as models for past societies that practiced agriculture and animal husbandry (e.g., Rogers et al., 2012; Saqalli et al., 2014; Riris, 2018; Verhagen et al., 2021; Vidal-Cordasco and Nuevo-López, 2021; Boogers and Daems, 2022), and for hunter-gatherer groups (e.g., Lake, 2000; Reynolds et al., 2006; Santos et al., 2015; Scherjon, 2019; Wren and Burke, 2019). In the case of ABM developed to study foragers, the use of fire by hunter-gatherers to transform foragers' habitats and the landscape consequences of these practices are usually not discussed (except for brief mentions of fire in some ABM case studies such as Ch'ng and Gaffney, 2013; Snitker, 2018).

The goal of this study is to investigate multiple drivers of change within a system-based approach, including fire (natural and human-induced), herbivory and climatic impacts. In this study we develop a new spatially explicit ABM (HUMLAND: HUMan impact on LANDcapes) whose specific focus is the impact of hunter-gatherers on vegetation. To demonstrate the potential of our approach, we applied it to a 500-year long time interval from the Early Holocene (9200–8700 BP), drawing on novel datasets produced as part of a wider body of research (Arthur et al., 2023; Davoli et al., 2023; Serge et al., 2023; Zapolska et al., 2023a). Despite recognizing the challenges posed by plant migration and other processes linked to glacial/interglacial transitions during the Early Holocene (e.g., Giesecke et al., 2017; Dallmeyer et al., 2022), we deliberately chose this time interval, preceding the widespread adoption of agriculture in Europe (Milisauskas, 2002; Gronenborn and Horejs, 2021; Hamon and Manen, 2021). This choice aligns with our primary focus on vegetation burning conducted by hunter-gatherers. Our study emphasizes the comparison of digital vegetation model outputs with pollen-based reconstructions, and their integration into the HUMLAND ABM. Additionally, the study incorporates continental-scale estimates of fire return intervals (FRI) and speed of vegetation regrowth in the current simulation, which were recently obtained specifically for this research. The article addresses the following sub-questions: 1) is it possible to create a modelling approach suitable for tracking and quantifying the intensity of different types of impact on interglacial landscapes at the continental level; 2) what defines the intensity of hunter-gatherer impact on interglacial vegetation?

2. Material and methods

2.1. Datasets used in the HUMLAND ABM

The simulation incorporates several datasets (Table 1). To standardize their spatial extent and resolution, Spatial Analysts and Data management ArcMap 10.6.1 toolboxes were used. The grid cell size of the input datasets was resampled to a common 10 km spatial resolution via the "Resample" tool of the "Data management toolbox" with the "Nearest neighbor" resampling method.

The initial landscape before simulation runs (Fig. 1) was constructed via the following datasets: Global Topography 30 Arc-Second elevation dataset (GTOPO30), Water Information System for Europe (WISE) and three outputs of a dynamic vegetation model CARbon Assimilation In the Biosphere (CARAIB) (Warnant et al., 1994; Gesch et al., 1999; Otto et al., 2002; Laurent et al., 2008; Danielson and Gesch, 2011; Dury et al., 2011; François et al., 2011). GTOPO30 is a digital elevation model (DEM) derived from several raster and vector sources of topographic information. We used this DEM to represent elevation data in the ABM. WISE is based on the information from the Water Framework Directive database. We assumed that this dataset represents distribution of major rivers and lakes during the study period, and we used these water bodies as natural barriers for the spread of fire in the model.

In the context of this research, the CARAIB dataset represents theoretical potential natural vegetation (PNV) distribution, driven by climatic conditions only (Zapolska et al., 2023a). As an input climate for running the CARIAB model, we used climatic variables simulated by the iLOVECLIM model (Goosse et al., 2010), revised by Roche (2013) and further expanded by Quiquet et al. (2018) with embedded online interactive downscaling (ibid.). Prior to the use of the iLOVECLIM-simulated climatic variables in the CARAIB model, they were bias-corrected using the Cumulative Distribution Function-transform (CDF-t) bias correction technique (Vrac, 2018; Zapolska et al., 2023b) and averaged over the studied period to get daily mean climate characteristics of our period of interest. CDF-t was selected as the bias-correction method, as it had demonstrated in previous testing within our specific setup (Zapolska et al., 2023b). CDF-t can be seen as an extension of the quantile-mapping (QM) method, allowing to account for climate change. As such, CDF-t mostly preserves the mean change of the variables to be corrected and, thus, behaves as the delta method in terms of means. As reference climate at present day for CDF-t calibration we used the EartH2Observe, WFDEI and ERA-Interim data Merged and Bias-corrected for the InterSectoral Impact Model Intercomparison Project (Lange, 2019). The CARAIB output dataset, used in this study, was previously published by Zapolska et al. (2023a), along with a full description of the modelling setup and the application of the CDF-t technique within this setup (Zapolska et al., 2023a, 2023b).

CARAIB outputs used in this study (Table 2) include distribution of fractions of 26 plant functional types (PNV PFTs), vegetation openness (PNV openness), leaf area index (LAI) and net primary productivity (PNV NPP) for the period 9200–8700 BP. Before being imported to the ABM, the mentioned CARAIB outputs were transformed (section 2.2). As the CARAIB dataset here represents climate-only forced vegetation, it is used in the current ABM as the starting point (i.e., before impact of

Table 1
Datasets used in HUMLAND.

Dataset	Initial data type	Initial spatial resolution/scale	Meaning, units	Source
GTOPO30	Raster	1 km	Digital elevation model, m	https://www.usgs.gov/
WISE	Vector	1:10,000,000	Distribution of large rivers and lakes	https://water.europa.eu/
CARAIB first dominant PFT	Raster	~26 km (0.25°)	PNV: first dominant PFT	http://www.umccb.ulg.ac.
CARAIB vegetation openness			PNV: vegetation openness (%)	be/Sci/m_car_e.html
NPP			PNV NPP (excluding carbon used for respiration), g/m^2	
Megafauna vegetation consumption	Raster	30 km	Potential maximal megafauna vegetation consumption (i.e., metabolization of NPP), kg/km^2 (converted to g/m^2)	Davoli et al., 2023
REVEALS first dominant PFT	Vector	~100 km (1°)	Observed first dominant PFT	Serge et al., 2023
REVEALS vegetation openness			Observed past vegetation openness (relative %)	
REVEALS vegetation openness standard errors			Standard errors for estimates of observed past vegetation openness	

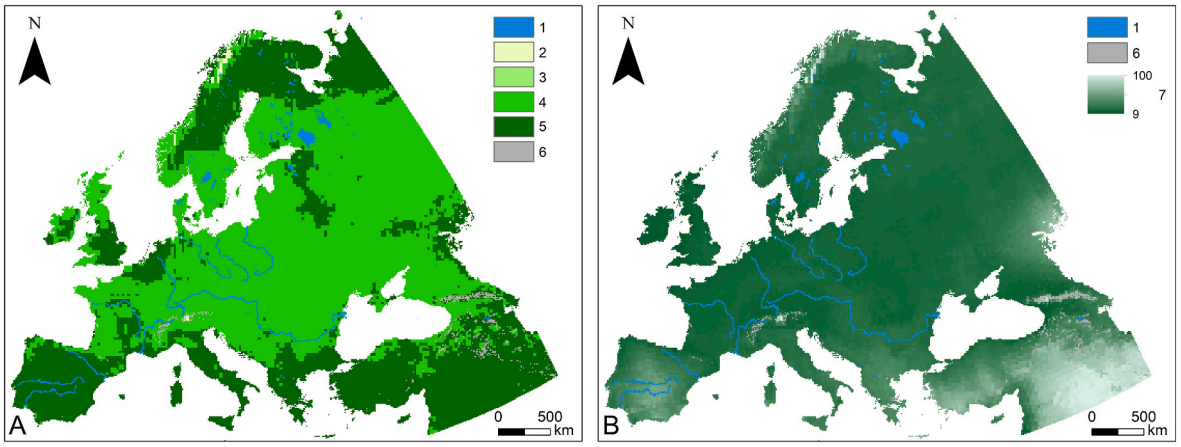

Fig. 1. The reconstructed environment prior to the HUMLAND simulation runs for 9200–8700 BP: distribution of first dominant HUMLAND PFTs (A) and vegetation openness (B). Legend: 1–large rivers and lakes; 2–herbs; 3–shrubs; 4–broadleaf trees; 5–needleleaf trees; 6–high mountains; 7–vegetation openness in percentages.

humans, natural fires and megafauna) of each simulation and as target for vegetation regrowth after impacts (section 2.3).

To include megafauna (wild terrestrial mammals≥10 kg) impact on vegetation in our study, we calculated potential maximal vegetation consumption of the wild herbivore communities across the continent, as they were distributed and diversified prior to the extensive influence of humans. For this, we used the present-natural ranges estimated by Faurby and Svenning (2015), which were downscaled to a 30 × 30 km grid-cell resolution by Davoli et al., 2023. Present-natural ranges are global estimates of mammal species distribution under climatic conditions similar to the Holocene. These ranges would be if *Homo sapiens* disturbance never occurred. In Davoli et al. (ibid.), these downscaled reconstructions were compared to species distribution reconstructions for the Last Interglacial to estimate differences between the two periods due to climate variability. The Early Holocene species pools were composed only of species occurring in Europe during this period in accordance with recent studies (Sommer, 2020). We considered these species pools and their distribution as representative of the potential maximum diversity of European herbivores in Early Holocene-like conditions without human impact, notably excluding species that went extinct in the Late Pleistocene, disregarding the reason for their extinction. Other comparable estimations of species distribution for the Early Holocene are not available, as the fossil record database is inherently scattered which potentially can lead to underestimation of faunal diversity (Crees et al., 2019). In the geographic space, we coupled the species pools with allometric estimates of plant consumption, in the form of consumed kg/km^2 per year per species at 30 × 30 km resolution (Davoli et al., 2023). The methodology to reconstruct these values is extensively described by Davoli et al. (ibid.). After summarizing the vegetation consumption per species for all the species present, we obtained estimates of total megafauna potential maximal plant consumption, which were integrated with PNV NPP into the ABM to determine the extent to which vegetation changed as a result of potential megafauna impact (section 2.3.4).

Simulation outputs and CARAIB vegetation openness and distribution of first dominant PFTs were compared against proxy records of vegetation composition for the period 9200–8700 BP (section 2.2). Among existing empirical proxies of past vegetation, pollen records from lake sediments or peat deposits have the best potential for quantitative reconstructions of plant abundance. Regional Estimates of Vegetation Abundance from Large Sites (REVEALS) (Sugita, 2007) is the only method so far that corrects the non-linear pollen–vegetation relationship by accounting for plant taxon-specific differences in pollen production, dispersal, and deposition (Prentice and Webb III, 1986; Sugita, 2007). It provides estimates of plant cover (in cover percentage of a defined area) for individual taxa. In recent years, datasets of pollen-based REVEALS plant cover were produced at a 1° × 1° grid cell spatial scale for large regions of the world, i.e., Europe, China, and North America–Canada (Trondman et al., 2015; Marquer et al., 2017; Cao et al., 2019; Githumbi et al., 2022; Li et al., 2023; Serge et al., 2023). Our study used REVEALS results from the most recent synthesis, which drew on a substantial number of pollen records (n = 1607) distributed across Europe (Serge et al., 2023). The dataset originally contains REVEALS estimates for 31 taxa, 25 consecutive time windows across the Holocene (11,700 BP–present), and 539 1° × 1° grid cells. For each cell, the REVEALS model has been run on all available pollen records (large and small pollen sites), and the mean REVEALS estimates of plant cover (and their standard errors) for the grid cell have been calculated for the 31 plant taxa (Table 2). The total cover of plant taxa within a grid cell is 100%. REVEALS cannot estimate the proportion of bare ground. The

Table 2
PFTs used in ABM (HUMLAND PFTs) and correspondence between CARAIB PFTs and REVEALS plant taxa.

CARAIB PFTs	Plant taxon/pollen morphological types	HUMLAND PFTs
Needleleaved evergreen boreal/temp cold trees	*Abies*	Needleleaf trees
Needleleaved evergreen meso mediterranean trees	*Picea*	
Needleleaved evergreen subtropical trees	*Pinus*	
Needleleaved evergreen supra mediterranean trees	*Juniperus*	
Needleleaved evergreen temperate cool trees		
Needleleaved summergreen boreal/temp cold trees		
Needleleaved summergreen subtropical swamp trees		
Broadleaved evergreen meso mediterranean trees	*Alnus*	Broadleaf trees
Broadleaved evergreen subtropical trees	*Betula*	
Broadleaved evergreen thermo mediterranean trees	*Carpinus betulus*	
Broadleaved evergreen tropical trees	*Carpinus orientalis*	
Broadleaved raingreen tropical trees	*Castanea sativa*	
Broadleaved summergreen boreal/temp cold trees	*Corylus avellana*	
Broadleaved summergreen temperate cool trees	*Fagus*	
Broadleaved summergreen temperate warm trees	*Fraxinus*	
	Phillyrea	
	Pistacia deciduous *Quercus* t.	
	evergreen *Quercus* t.	
	Salix	
	Tilia	
	Ulmus	
Broadleaved evergreen boreal/temp cold shrubs	*Buxus sempervirens*	Shrubs
Broadleaved evergreen temperate warm shrubs	*Calluna vulgaris*	
Broadleaved evergreen xeric shrubs	Ericaceae	
Broadleaved summergreen arctic shrubs		
Broadleaved summergreen boreal/temp cold shrubs		
Broadleaved summergreen temperate warm shrubs		
Subdesertic shrubs		
Tropical shrubs		
C3 herbs (“dry”)	Amaranthaceae/Chenopodiaceae	Herbs
C3 herbs (“humid”)	*Artemisia*	
C4 herbs	Cerealia t.	
	Cyperaceae	
	Filipendula	
	Plantago lanceolata	
	Poaceae	
	Rumex acetosa t.	
	Secale cereale	

protocol for grid system, pollen data handling and REVEALS application was previously published (Mazier et al., 2012; Trondman et al., 2016; Githumbi et al., 2022).

The REVEALS dataset for the studied time window (9200–8700 BP) represents observed past vegetation cover, and, therefore, reflects vegetation cover impacted by all possible drivers, including megafauna, climate, anthropogenic and natural fires. In HUMLAND, REVEALS data is used as a target vegetation cover for the simulation output. Before being imported to HUMLAND, the used REVEALS and CARAIB outputs were transformed (section 2.2).

2.2. CARAIB, REVEALS and ABM output comparison

CARAIB and REVEALS are different modelling approaches, with dissimilar outputs (section 2.1). The similarity between the two datasets is that they both produce quantitative output: CARAIB generates distributions of fractions for 26 PFTs, and REVEALS provides proportions for individual taxa. The outputs of these models were compared in terms of vegetation openness and distribution of first dominant PFTs in the study area.

Currently, there is no accepted protocol for comparing the CARAIB and REVEALS models and for integrating them into a single ABM. Therefore, prior to the comparison of dominant PFT distributions and their incorporation into HUMLAND, the datasets were transformed (i.e., reclassified) into categorical (qualitative) descriptions of dominant PFTs. Here we applied a classification approach described by Zapolska et al. (2023a), based on classification by Popova et al. (2013) and Henrot et al. (2017), which was further organized into four general categories: herbs, shrubs, needleleaf trees and broadleaf trees (Table 2).

The definition of common categories which would be relevant for both datasets on the continental scale is rather complex. These categories were chosen because both datasets contain information about types of plants (herbs, trees, and shrubs) and leaf types of present woody plants. Furthermore, the primary focus of the current study is the impact of fire on vegetation, and, therefore, the ABM classification should reflect differences in vegetation responses to fires. Needleleaf trees and broadleaf trees are generally characterized by different degrees of flammability. Coniferous forests are fire-prone communities because the crowns of trees are often densely packed, have low moisture levels, and litter accumulates due to low decomposition rates (Bond and Wilgen, 1996). Deciduous plants are usually less flammable in comparison with coniferous species, mainly because living leaves have higher moisture content (Doran et al., 2004). Herbaceous plants such as grasses are easily ignited and burn rapidly during most of the year (Dennis, 1999), because dieback of grass leaves can produce a dense litter layer (Bond and Wilgen, 1996). Shrubs are generally flammable, because they often grow in dense groups or thickets (Doran et al., 2004). As a result, shrublands can be subject to intense crown fires because of their higher fuel loads (Bond and Wilgen, 1996). Thus, CARAIB and REVEALS PFTs are included in the current simulation and compared in terms of four general categories of the first dominant PFTs: needleleaf and broadleaf trees, shrubs and herbs. While the CARAIB model provides output in PFTs directly, REVEALS PFTs were calculated by summing the mean relative percentage cover of each associated taxon (Table 2).

After both datasets were reclassified, we calculated F1-score for their distribution of general PFTs used in HUMLAND. The F1-score is a metric often used to assess the accuracy of a classification model in machine learning. This value combines both precision (the accuracy of positive

predictions) and recall (the model's ability to correctly identify all relevant instances). F1-score ranges between 0 and 1, where 1 represents perfect precision and recall, and 0 represents the worst performance.

Besides the first dominant PFT, we used CARAIB PNV and REVEALS outputs in terms of potential natural (CARAIB) and observed (REVEALS) vegetation openness in percentages. However, these two datasets estimate vegetation openness in a different way (Fig. S1 showing these differences is available in Appendix A Supplementary data).

Vegetation openness in REVEALS was estimated via the percentage of an open land (OL) land-cover type, which combines the percentage of all herbs (Table 2) and *Calluna vulgaris* (Trondman et al., 2015; Serge et al., 2023). Since REVEALS estimates are based on pollen data, this approach cannot account for bare ground. However, REVEALS provides estimates of standard error values (uncertainties of the averaged REVEALS estimates) for every plant taxon per grid cell using the delta method (Stuart and Ord, 1994), based on the methodology from Sugita (2007). Standard errors were obtained from the sum of the within- and between-site variations of the REVEALS results per grid cell (Githumbi et al., 2022). Therefore, it is possible to estimate the quality of data, and calculate possible maximal and minimal values for vegetation openness.

In CARAIB, simulated PFTs can co-exist on the same grid, forming two vertical levels: upper (trees) and lower (shrubs, herbs and bare ground). The primary focus of this study is on human activity. We therefore attributed bare ground and grass to open landscapes, and trees and shrubs to closed landscapes, based on the ability of each plant group to restrict human activity (e.g., human movements are impeded by closed vegetation dominated by shrubs or trees; and it is easier to move within open landscapes dominated by herbs). The maximum possible openness value for each of the two vertical CARAIB levels is 100% (i.e., the percentage of a level not covered by shrubs or trees), and, therefore, the maximum possible value for each grid cell is 200% (i.e., vegetation is completely open because only bare ground and/or herbs are present). Vegetation openness was first calculated for trees and shrubs separately, using formula (1):

$$\text{Monthly openness} = e\text{^}(-0.5 * \text{LAI}) \quad (1)$$

where e–exponential constant, approximately equal to 2.718, and LAI–leaf area index for each month (leaf area/ground area in m^2/m^2).

Minimal Monthly openness represents vegetation at its full growth potential. Therefore, the minimum value of monthly openness per grid cell was used for further calculations. Because the REVEALS dataset provides one vegetation openness value per grid cell, we also assigned one CARAIB vegetation openness value to each grid cell. Under the assumption that upper and lower PFTs spatially align within a grid cell, we assumed the smaller openness value among the two to be representative of grid cell vegetation openness, as it indicates a fraction of an area where neither upper (trees) nor lower (shrubs) vegetation is present. As a result, both CARAIB and REVEALS have one vegetation openness value per grid cell. A two-sample t-test was applied to 500 randomly selected cells with both REVEALS and CARAIB vegetation openness estimates. The t-value is a measure used to assess whether the difference between the means of two groups is significant or if it could have happened by random chance.

In HUMLAND, more closed vegetation can only switch to more open vegetation after a disturbance event (e.g., fire, grazing). In our data comparison, where CARAIB shows a greater degree of openness in vegetation than REVEALS, we exclude these locations: the ABM will not be able to generate vegetation that is comparable to REVEALS as it is constrained by the CARAIB-prescribed PNV. As a result, the similarity between ABM output and REVEALS datasets can only be improved for grid cells where initial vegetation openness is equal to or lower than observed estimates. Secondly, there are several grid cells where climatic conditions only favor dominance of herbs or shrubs, but observed vegetation indicates dominance of trees. Besides that, shrubs cannot dominate grid cells where climatic conditions favor trees or herbs in HUMLAND. Such cases do not improve similarity between ABM output and REVEALS data, and, therefore, these grid cells were also excluded (Table S2 with more explanations about conflicting grid cells is available in Appendix A Supplementary data).

After the CARAIB and REVEALS datasets were imported to HUMLAND and conflicting grid cells were excluded, the mean percentage of each first dominant PFT and mean vegetation openness was calculated for all remaining grid cells with both CARAIB and REVEALS estimates. These mean values were used during ABM runs to assess the performance of the model, and to identify simulation runs which produced results similar to REVEALS. ABM outputs are considered similar to REVEALS estimates if the difference in the mean percentage of each first dominant PFT and mean vegetation openness does not exceed ±5% (the range of change is 10%). For such ABM outputs, we calculated F1-scores and t-values. These measures for ABM outputs and the CARAIB–REVEALS comparisons were obtained using ArcMap 10.6.1 and R (RStudio Version 1.3.1093, R Core Team, 2020) with the *caret* (Kuhn, 2008) and *tidyverse* (Wickham et al., 2019) packages.

2.3. Agent-based model

The current continental ABM was implemented in NetLogo 6.2.2 (Wilensky, 1999). The temporal resolution of the model is one year, and, therefore, seasonality is out of the scope of our research. Due to that and the spatial resolution of the model (10 km), many types of impact on vegetation (e.g., droughts, cooling, and insect activity throughout a year) and the seasonal movements of hunter-gatherers are beyond the scope of this paper.

This model does include four types of impact on vegetation: climate, anthropogenic fires, thunderstorms, and megafauna plant consumption (activity diagram can be found in Appendix A Supplementary data, Fig. S3). Thunderstorms were included because lightning is one of the most general and widespread triggers of natural fire (Whelan, 1995). Another source of impact is climate, and it is included as a crucial element for vegetation regeneration after fires or vegetation consumption (section 2.3.1). Finally, megafauna are also a part of the current ABM, because their activity impacts litter accumulation, and high levels of megafauna plant consumption reduce fire occurrence in many areas (Bond and Wilgen, 1996; Pringle et al., 2023). Simulation stops after 1000 steps.

2.3.1. Climatic impact

Each simulation step starts with climatic impact, which defines vegetation regrowth after fire events or megafauna vegetation consumption. Fire effects on vegetation and vegetation regrowth are difficult to predict due to variability of plant composition and fire characteristics such as frequency, intensity, and size (Zwolinski, 1990; Johnson and Miyanishi, 2021). Consequences of burning can vary from minor (e.g., fire scars and scorches) to complete vegetation replacement (Kleynhans et al., 2020). Due to the large study area, 10 km resolution and the primary focus on anthropogenic burning in the current model, all burning events replace vegetation of a grid cell by bare ground in HUMLAND. The mean number of years to recover is used to define the rate of vegetation regrowth after fires or vegetation consumption.

In the course of our research, we did not find estimates for the mean number of years to recover for four broad PFT categories used in this study (Table 2). Due to that, the mean number of years to recover was calculated via CARAIB. First, a maximum of five representative grid cells for each of 26 CARAIB PFTs (Table 2) were chosen. For the PFTs where less than five grid cells were found to be representative, we selected all the existing cells. A grid cell is representative if a selected PFT did not experience any evident competition with other PFTs within the grid cell, and after a certain number of years stabilized into an equilibrium state of dominance on the grid cell. Thus, extracted periods represent the number of years needed for a PFT to grow from the bare ground and establish as a dominant PFT on a grid cell in CARAIB.

After that, CARAIB PFTs were reclassified as four HUMLAND PFTs in accordance with Table 2, and we created frequency histograms for each of the general PFT categories. These histograms were analysed and outlier values were excluded. Afterwards, the mean values were calculated for each general PFT. These values represent the number of years which is required for each PFT to recover as it was before the fire episode or complete vegetation consumption by megafauna: seven years for herbs, 43 years for needleleaf trees and shrubs, 30 years for broadleaf trees.

Vegetation regrowth occurs for both dominant PFTs and vegetation openness. The first step of PFT recovery in ABM always starts with herbs, which replace bare ground after seven simulation steps in the model. Afterwards, herbs could be replaced by trees or shrubs in accordance with an initial dominant PFT estimated by CARAIB after the required mean number of years to recover.

Rate of vegetation openness recovery rate (V_{or}) is calculated in formula 2:

$$V_{or} = \frac{O_i - O_c}{\mu} \quad (2)$$

O_i is vegetation openness after impact done by fire or megafauna; O_c–CARAIB estimates of vegetation openness; and μ–mean number of years required for recovery of the initial vegetation openness before fire event or plant consumption. Every simulation step V_{or} is subtracted from current simulation openness until it reaches CARAIB vegetation openness estimates.

2.3.2. Anthropogenic fires

Humans impact landscapes after vegetation regrowth. There are five parameters which define human behavior and the intensity of their impact: number of hunter-gatherer groups, accessible radius, campsites to move, their movement frequency, and openness criteria to burn. After human-induced burning, fire can spread depending on the probability of ignition of neighboring cells (section 2.3.3).

The first parameter defines the number of groups in the study area during one simulation run, and, therefore, this parameter is associated with human population size. There are studies focused on relationships between fire regime, frequency and human population size in the past and the present at different spatial scales (e.g., Bistinas et al., 2013; Knorr et al., 2014; Sweeney et al., 2022). It was shown that both positive and negative relationships can vary from continent to continent (Bistinas et al., 2013). Such studies rarely focus on periods when foraging was the dominant subsistence strategy. Given the ambiguous nature of the relationships and the uncertainty surrounding the inclusion or exclusion of this parameter, we ultimately included it in HUMLAND. In the current model, one moving agent represents the whole group. The initial distribution of groups and their campsites is random at the beginning of each run. Humans cannot occupy and move on water bodies and high mountains (i.e., elevation above 2500 m a.s.l.).

The accessible radius parameter defines the territory within which humans move and set fires around campsites. In accordance with Binford's model (Binford, 1982), the area around hunter-gatherer sites includes a foraging radius and a logistical radius. The first one defines the area where most resources are obtained, and this zone rarely exceeds ~10 km (ibid.). The second radius defines the area used by task groups e.g., for raw material procurement or food collecting, special activities that could imply staying away from "base camp" from one night to much longer periods (e.g., hunting for four weeks or three months) (ibid.). The accessible radius parameter in HUMLAND defines the territory which includes both foraging and logistical radii. If the parameter value is set to 0, the group does not move from their basecamp site, and only impacts the grid cell where this campsite is located. Higher parameter values expand the accessible radius (e.g., accessible radius 3 would allow humans to move within 3 grid cells radius, ~40 km around their campsites including the grid cell with a campsite on it).

Due to the importance of seasonal movements for the hunter-gatherer lifestyle (Kelly, 2013), there are two parameters associated with the movements of campsites: Movement_frequency_of_campsites (the number of simulation steps after which groups can relocate a campsite) and Campsites_to_move (the percentage of hominin groups that relocate a campsite at certain step). Given the temporal resolution of the current simulation, hunter-gatherers' highest possible frequency of camp movements is every step (i.e., once per year). The search radius for the new grid cell to establish a site is twice the accessible radius. Any grid cell can be chosen for the new site, except the previously occupied one. The newly established accessible area can overlap with the previous one.

Since hunter-gatherers have different reasons to burn landscapes, and that this practice was documented in almost all vegetation types with more cases for foragers occupying shrublands and forests (Mellars, 1976; Scherjon et al., 2015), the openness criteria to burn was introduced. In the current simulation, humans only burn patches dominated by trees or shrubs with vegetation openness lower or equal to this criterion. Its low values minimize the number of positive decisions to start fire, and higher values increase human-induced fires, because even relatively open areas can be burnt by people in this case.

2.3.3. Thunderstorms

The model contains the parameter which defines the number of thunderstorms per simulation step. They randomly appear on grid cells within the study area. Fire starts depending on the probability of ignition of these cells. Fire can spread on the neighboring grid cells following both human-induced and natural fires, and this process depends on the probability of ignition. In other words, thunderstorms do not always cause vegetation burning, and fire does not always spread after natural and human-induced ignitions. Thunderstorms can appear over water bodies and high mountains, but these areas cannot be burnt, and, therefore, they are natural barriers for fire.

The probability of ignition P(I) is calculated in formula (3). P(I) depends on time passed since the last burning episode (B) and natural FRI (F).

$$P(I) = \frac{T - B}{F} \quad (3)$$

T corresponds to the number of simulation steps (ticks) since the beginning of the simulation.

Estimating accurate FRI values requires long-term observations spanning multiple fire episodes over time. Globally, FRI can range from sub-annual values in frequently burning savannas to 1000 years or more in some temperate and boreal regions (Harrison et al., 2021). While direct observations over such long periods do not exist, indirect estimates can be derived by measuring char layers in sediment cores, ice cores, and tree rings. However, the spatial coverage of such estimates is limited. Another method to gain more insight in spatial patterns is by the use of so-called "space-for-time" substitution, based on remote sensing data of fire activity (Archibald et al., 2013). We used this substitution method to estimate the average fire-return interval for each 0.25° grid cell. It is assumed that the spatial and temporal variability in fire events is equal within a given grid cell, which allows for the interpretation of the spatial distribution of fire events as a measure for the temporal return time. For example, if a grid cell has burned for 25% in 20 years of the available satellite observation record, the resulting FRI is 20/0.25 = 80 years. In frequently burning savanna regions a grid cell could burn almost entirely each year, giving an FRI close to 1 year.

We used 2002–2020 MODIS burned area (BA) data from the MCD64A1 C6 product (Giglio et al., 2018) to calculate satellite-derived approximated FRI for four HUMLAND PFTs used in the current ABM. These PFTs were demarked using the annual PFT classification from the MCD12Q1 C6 land cover type product (Friedl and Sulla-Menashe, 2019). Evergreen and deciduous needleleaf forest classes were grouped as needleleaf trees, and evergreen and deciduous broadleaf forest classes were grouped as broadleaf trees. For each HUMLAND PFT, we

first calculated the sum of 20 years of BA for each 500 m pixel, i.e., the fire frequency. We then calculated the average annual BA for each 0.25° grid cell by aggregation of the 500 m values. The FRI followed, by taking the reciprocal of the average annual BA. Afterwards, FRI values were obtained for grid cells where all four PFTs were present, and histograms of frequency distribution were created and analysed. Based on gaps and clear gradients between values on the histograms, the lowest and the highest FRI values were identified. These values were excluded, because we assumed that they reflect modern, relatively frequent fire use or delayed fire frequency due to fire management. For the remaining values, the mean FRI was calculated for each dominant PFT: 293 years for herbs, 286 for shrubs, 426 for broadleaf trees, and 246 for needleleaf trees. The obtained estimates were compared against the existing estimates derived from sediment sites dated to the Early–Middle Holocene in Europe (Pitkänen et al., 2001; Vannière et al., 2008; Feurdean et al., 2013; Feurdean et al., 2017; Novenko et al., 2018; Feurdean et al., 2019; summary of estimates from sediment sites can be found in Appendix A Supplementary data, Table S4).

2.3.4. Megafauna vegetation consumption

Megafauna constitutes the last agent which causes vegetation transformation in the model per simulation step. Only grid cells with fully recovered vegetation can be consumed by megafauna in HUMLAND. This assumption arises from our use of estimates for potential maximal megafauna plant consumption and the absence of data regarding partial consumption during the vegetation regrowth phase. After plant consumption, vegetation openness increases depending on the CARAIB NPP values and the maximal megafauna plant consumption estimates. We explicitly note that this assumption will underestimate megafauna impacts on vegetation regeneration in HUMLAND.

As our research primarily focuses on continental-level patterns for four broad PFT categories (Table 2), our analysis is conducted at a higher ecological scale than the plant taxon level. As a result, it is assumed that megafauna equally consume all PFTs present on a grid cell, i.e., besides the first dominant PFT megafauna consume the second, third and fourth dominant PFTs in equal proportions. Therefore, the first dominant PFT is replaced only if the vegetation was entirely consumed by megafauna and the vegetation openness value after consumption is 100%. In this case, the first dominant PFT would be replaced by bare ground.

The percentage of consumed vegetation (V_c) is calculated for each grid cell excluding water bodies and high mountains via formula (4):

$$V_c = \frac{V_m}{V_n} \times 100 \quad (4)$$

V_m and V_n values are obtained from datasets: V_m is a grid cell value for megafauna metabolization of NPP, and V_n is CARAIB NPP. After calculating the percentage of consumed vegetation in a grid cell, this value is combined with the vegetation openness value to enhance it following megafauna impact. The percentage of consumed vegetation influences the timing of reaching 100% in P(I) and, as a result, the effects of vegetation change caused by fires can be postponed due to consumption. Finally, the update of the first dominant PFT depends on the resulting vegetation openness achieved after vegetation consumption.

2.4. Experiments, observations, and analysis

The primary observations made during simulation runs include the distribution of the first dominant PFTs (percentage of grid cells covered by each of four general PFTs) and mean vegetation openness. We collected these observations only for grid cells that have both CARAIB and REVEALS values. The ABM output is considered similar to REVEALS data if the observations and REVEALS values vary within ±5% (the range of change is 10%).

Several sets of experiments were conducted, and every parameter combination had 30 runs whose outputs were analysed in R with the *ggplot2* (Wickham, 2016) and *tidyverse* (Wickham et al., 2019) packages. The adequacy of this number of runs is underscored by the minimal standard deviation observed across nearly all outputs (standard deviation values are in Tables S6, S8, S9, S13, and S14 of Appendix A Supplementary data).

During the first set of experiments, vegetation had only two types of impact: humans and climate; megafauna and climate; thunderstorms and climate. The main objective of these experiments was to isolate the impact of humans, megafauna, and natural fires, in order to determine whether it was possible to achieve REVEALS estimates without considering all agents together. Furthermore, this also served to establish the number of simulation steps required to reach equilibrium (i.e., state of a simulation when the values for primary observations do not significantly change anymore). During the first set of experiments, we also identified the highest achievable parameter values, as these are only attainable when exclusively one of the three impact types–megafauna, anthropogenic, or natural fires–is operative, leading to outcomes similar to REVEALS outputs. The identified maximum parameter values were integrated into the sensitivity analysis (see below).

Secondly, megafauna, thunderstorms, and climate impacted vegetation together. These experiments defined in which case the simulation reached the REVEALS estimate without any role of humans. Finally, all four types of impact were combined to conduct a sensitivity analysis, to produce potential scenarios, and to identify the most influential agent in continental-level vegetation change.

A sensitivity analysis was performed via the *nlrx* R package (Salecker et al., 2019) to understand what defines the intensity of human-induced vegetation changes. Sensitivity analysis was conducted via the Latin Hypercube Sampling (LHS) technique developed by McKay et al. (1979), and Iman and Conover (1980). This method ensures that each factor is represented in a balanced manner irrespective of their importance (Saltelli et al., 2004). The technique involves dividing the ranges of parameter values into equally probable intervals and then sampling from each interval to ensure a representative sample of the input space. In this study, we conducted one LHS run, as multiple runs would demand a substantial amount of time and computational resources. LHS set up had two random seeds, and collected 160 samples for each run. Then, we used Partial Rank correlation coefficient (PRCC) which is widely used in sensitivity studies to measure the strength of a linear association between input and output (Hamby, 1994; Marino et al., 2008).

Once the most influential factors for human-induced vegetation change were identified via LHS/PRCC, the minimum, midpoint (average) and maximum values for these parameters were used to identify the first potential scenarios of vegetation change. Each parameter combination had 30 runs. A two-sample t-test for 500 randomly selected cells was conducted, and the F-1 score was calculated for the REVEALS dataset and potential scenarios similar to REVEALS data.

3. Results

3.1. CARAIB and REVEALS datasets comparison

Out of the total 21,203 10 × 10 km grid cells with both REVEALS and CARAIB estimates, 25% of the grid cells were excluded from further analysis, as CARAIB predicts lower vegetation openness than the REVEALS results. Figs. 2 and 3 show data comparison results after importing these datasets to HUMLAND and excluding the conflicting grid cells. There are more grid cells with the primary dominance of trees in the CARAIB dataset (Fig. 2 A, B) than in REVEALS (Fig. 2 C, D). F1-score for these two datasets is 0.001 with accuracy 0.51. Regarding the vegetation openness, REVEALS shows a more open landscape in comparison with CARAIB estimates (Fig. 3). The mean values for vegetation openness are 43% and 20%, respectively (Fig. 3C), and the t-value = -20.85 for 500 randomly selected cells (p-value<2.2e-16, df = 998).

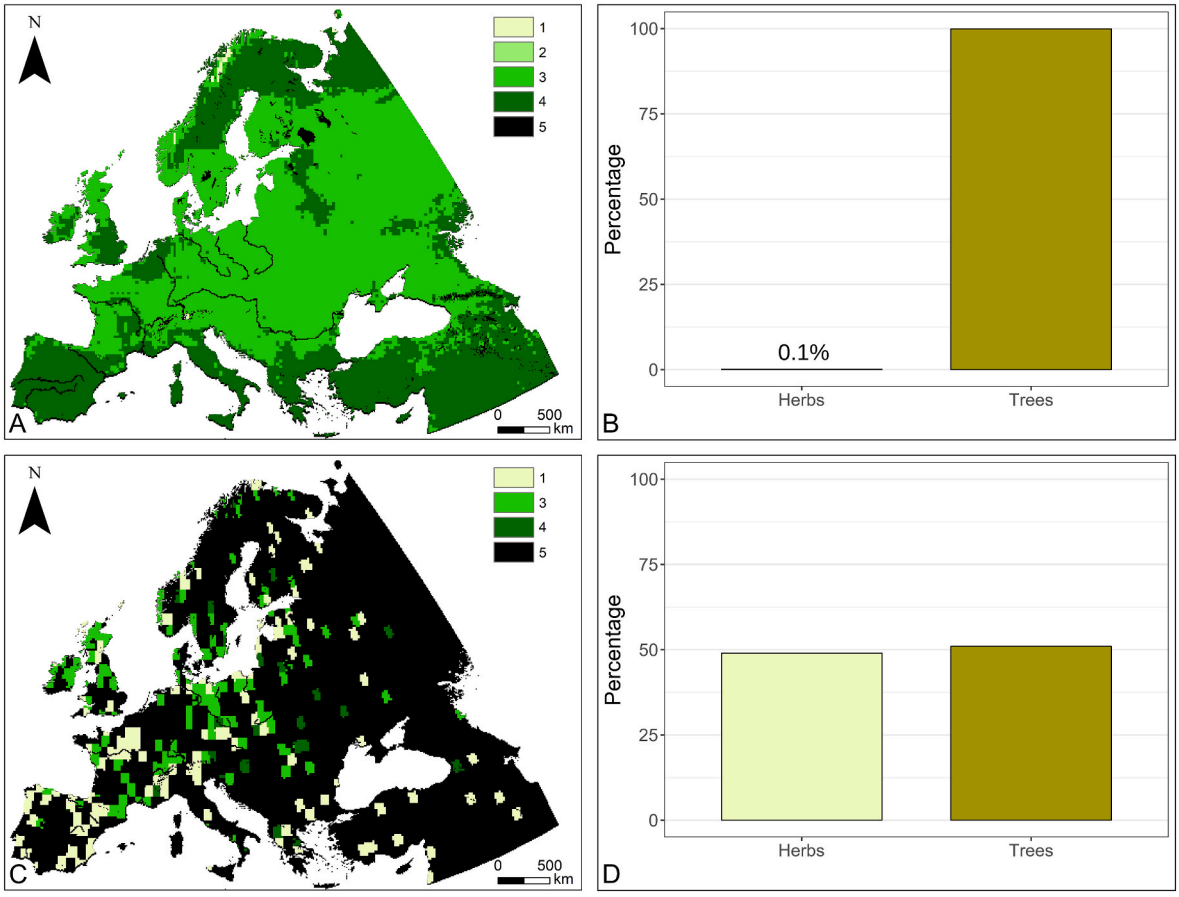

Fig. 2. CARAIB (A) and REVEALS (C) first dominant HUMLAND PFT distribution accompanied with bar graphs of the proportions (100% on the bar graphs equals the number of grid cells with both REVEALS and CARAIB estimates) of CARAIB (B) and REVEALS (D) after excluding the grid cells where CARAIB predicts lower vegetation openness than the REVEALS results. Legend: 1–herbs; 2–shrubs; 3–broadleaf trees; 4–needleleaf trees; 5–no data.

3.2. Natural fires and megafauna impact without human presence

The results of experiments when thunderstorms and megafauna impact separately without human presence showed that minimal impact of natural fires starts when 0.1% of all terrestrial cells have thunderstorms (Fig. 4 A, B). REVEALS trees (Fig. 4A) and vegetation openness (Fig. 4B) estimates are reached when 7% and 4.7% of all terrestrial cells are impacted by thunderstorms. These values are maximal for the parameter which defines the number of thunderstorms per simulation step. The equilibrium is reached after 450 steps (Fig. 4A and B).

The impact of megafauna plant consumption did not have a significant effect on the vegetation (Fig. 4C and D), because the percentage of consumed vegetation never exceeds 1%. The obtained modelling results thus show that megafauna does not significantly change the distribution of dominant PFTs and mean vegetation openness on the continental level. Due to the low intensity of megafauna impact, the experiments with a combination of the three types of impact (thunderstorms, climate and megafauna) did not lead to different maximal and minimal Territory_impacted_by_thunderstorms parameter values, in comparison to the results obtained when thunderstorms and climate impact vegetation without megafauna presence.

3.3. Anthropogenic impact on vegetation without natural fires and megafauna plant consumption

Several sets of experiments with only anthropogenic and climatic impacts were conducted to define maximal and minimal values for five parameters associated with human-induced vegetation change. Firstly, the Number_of_hunter-gatherer_groups parameter was varied, while others remained constant (Openness_criteria_to_burn = 50, Campsites_to_move = 50, Movement_frequency_of_campsites = 500, Accessible_radius = 5). Human induced vegetation changes start when there is only one group present (Fig. 5), and, therefore, this is the minimal value for this parameter. REVEALS openness estimates were reached when 3128 groups impact vegetation and REVEALS percentage of cells dominated by forest was reached with 3167 groups (Fig. 5). Thus, the maximum parameter value for Number_of_hunter-gatherer_groups is not lower than 3167.

Fig. 5 demonstrates a noticeable difference in simulation outcomes between the minimum (1) and maximum (3128 and 3167) values of the Number_of_hunter-gatherer_groups parameter, highlighting its significant impact on the model output. To further understand the impact of other parameters on the model output and track its behavior in relation to different human population sizes, we varied the parameters related to anthropogenic burning for 100, 1000, and 4000 groups. The experimental results for 4000 groups are presented in Fig. 6, as this value was determined to be the maximum parameter value. This was because the majority of simulation outputs for 4000 groups exceeded REVEALS estimates. The graphs with the results of experiments for 100 and 1000 groups can be found in the appendix.

The variation of values for Accessible_radius parameter produces different model outputs when this parameter is set to 5 or lower (Fig. 6A). The simulation results do not change significantly when the radius has higher values. Additionally, we found that the simulations reach their equilibrium after 200 to 300 steps.

The parameter Openness_criteria_to_burn must not be set lower than 9%, as this corresponds to the minimum threshold for vegetation openness of the CARAIB dataset (Fig. 1B). When this parameter is set to 58%

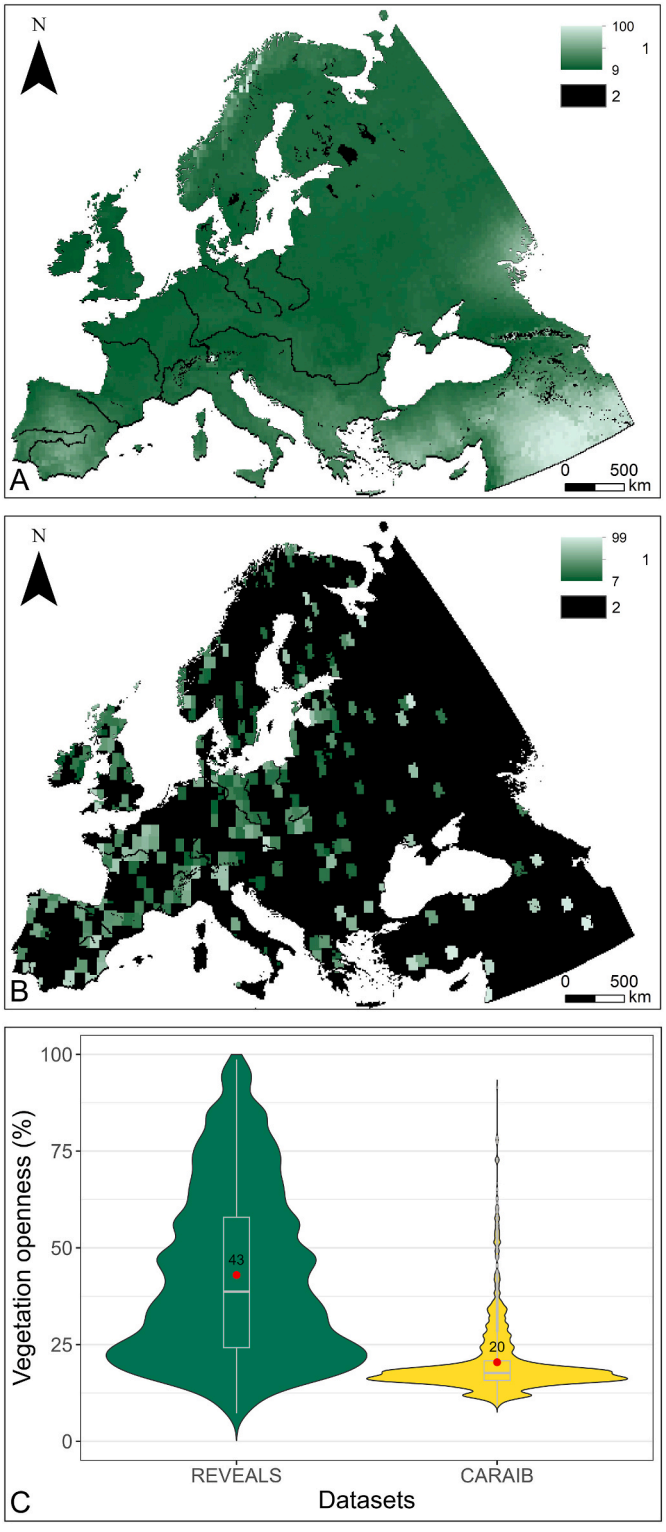

Fig. 3. Vegetation openness of CARAIB (A) and REVEALS (B) with a summary of these datasets and their values' distribution only for grid cells with both REVEALS and CARAIB estimates (C) after excluding the grid cells where CARAIB predicts lower vegetation openness than the REVEALS results. In subfigure C the dot indicates the mean value for each dataset. Legend: 1–vegetation openness in percentages; 2–no data.

the model output in terms of the mean percentage of cells dominated by trees does not change significantly. Similarly, the mean vegetation openness does not change significantly when Openness_criteria_to_burn is set to 46% (Fig. 6 C, D). Therefore, 58% is the maximum possible value for the Openness_criteria_to_burn parameter. After 300 steps, the simulations reach their equilibrium.

The results remain largely unaffected by variations in the Campsites_to_move parameter (Fig. 6 E, F), i.e., its low and high values produce similar results. On the contrary, values between 1 and 21 for the Movement_frequency_of_campsites parameter lead to different results (Fig. 6 G, H), and the equilibrium is reached after 200 steps. If this parameter has values higher than 21, the output does not vary.

As a result of this research step, the model behavior was examined in relation to climatic impact together with the separate impacts of each agent: humans, thunderstorms, megafauna, or the combination of the latter two. We identified the maximum and minimum parameter values, and the number of steps required to reach equilibrium. These estimates served as the foundation for setting up the sensitivity analysis.

3.4. Sensitivity analysis: combined impact of humans, megafauna, climate and natural fires on vegetation

Table 3 provides a detailed overview of the sensitivity analysis experiment that was undertaken to assess the extent to which different parameters influence the model outcomes. The analysis was based on the findings presented in Sections 3.2 and 3.3. Several parameter settings in the sensitivity analysis, such as Territory_impacted_by_thunderstorms, Accessible_radius, and Movement_frequency_of_campsites, correspond to the maximum and minimum values identified in these sections. We set the maximm value of Number_of_hunter-gatherer_groups to 4000, as experiments with separate impact of humans and climate revealed that this parameter's maximum value is not less than 3167, and most of the simulation outputs exceeded REVEALS results when this parameter was set to 4000. Experiments showed that the maximum value for the Openness_criteria_to_burn parameter varies greatly depending on the Number_of_hunter-gatherer_groups value. Due to this, Openness_criteria_to_burn was set to 100% in the sensitivity analysis to explore all possible combinations for this parameter with other settings. Moreover, we assigned 100% as the maximum value for Campsites_to_move to confirm that this parameter is relatively less important for HUMLAND output despite the value of this parameter.

The sensitivity analysis considers the combined impact of all agents, including constant presence of megafauna in all simulations. In Fig. 4, we identified the maximum starting point for equilibrium during simulations with the separate impact of each agent at step 450. As a result, we took the primary measurements–mean vegetation openness and the percentage of grid cells dominated by trees–between steps 450 and 1000 for the sensitivity analysis.

As we can see in Fig. 7, four parameters (Number_of_hunter_gatherer_groups, Accessible_radius, Openness_criteria_to_burn, and Territory_impacted_by_thunderstorms) have greater influence on the model output than parameters associated with campsites' movements (Campsites_to_move and Movement_frequency_of_campsites). All the parameters, except for Movement_frequency_of_campsites, exhibit PRCC values with p-values$<$0.05, indicating their statistical significance within LHS/PRCC analysis. Thus, the choice of 160 samples for two random seeds proved to be appropriate as it yielded statistically significant results. For the Movement_frequency_of_campsites parameter, the p-values are 0.17 (mean vegetation openness) and 0.14 (grid cells dominated by trees in percentage). While these p-values$>$0.05, it can still be concluded that its impact on the model output is relatively weaker. This is because the Movement_frequency_of_campsites parameter operates in conjunction with Campsites_to_move, and if it is set to 0%, the campsites will not be relocated regardless of their movement frequency.

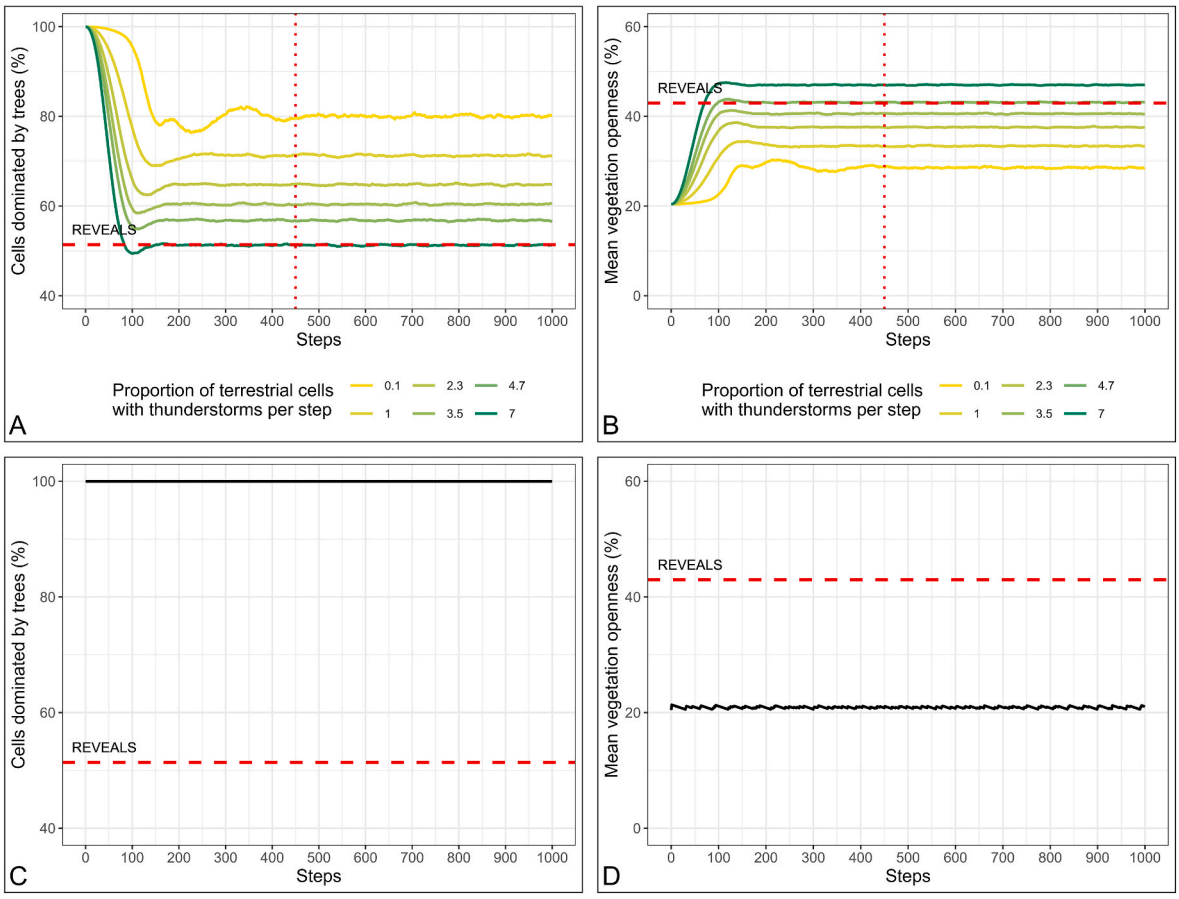

Fig. 4. Percentage of cells dominated by trees (A) and mean vegetation openness (B) after natural fires caused by thunderstorms and impact of climate, and percentage of cells dominated by forest (C) and mean vegetation openness (D) after megafauna vegetation consumption and impact of climate. Each line depicted on the experiment output graph represents the mean of 30 simulation runs. The horizontal dashed line indicates REVEALS estimates, and the vertical dotted line shows the step when simulations reach equilibrium.

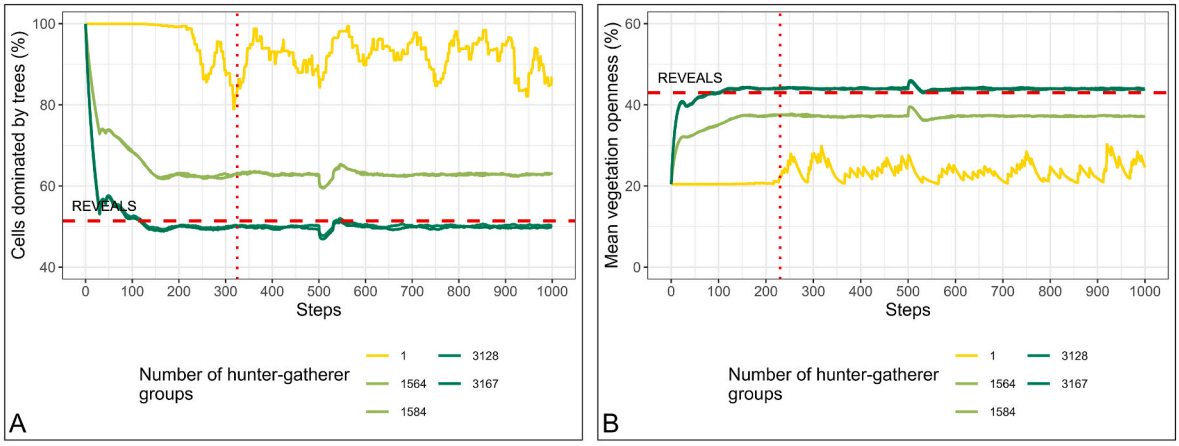

Fig. 5. Percentage of cells dominated by trees (A) and mean vegetation openness (B) caused by different numbers of hunter-gatherer groups and climatic impacts. Each line depicted on the experiment output graph represents the mean of 30 simulation runs. The horizontal dashed line indicates REVEALS estimates, and the vertical dotted line shows the step when simulations reach equilibrium.

4. Discussion

4.1. How much do pollen-based estimates correspond to climate-based vegetation cover?

Comparison of CARAIB and REVEALS datasets indicated a substantial difference between the two. Due to the low F1-score, they have poor agreement in terms of the first dominant PFTs distribution. Similar patterns came from the comparison of vegetation openness for these datasets. The results of the two-sample t-test showed that there is a substantial difference between them, and that the difference is unlikely to be due to random variation.

Since REVEALS and CARAIB are not "equal" models (i.e., REVEALS quantitatively reconstructs regional vegetation abundance from pollen

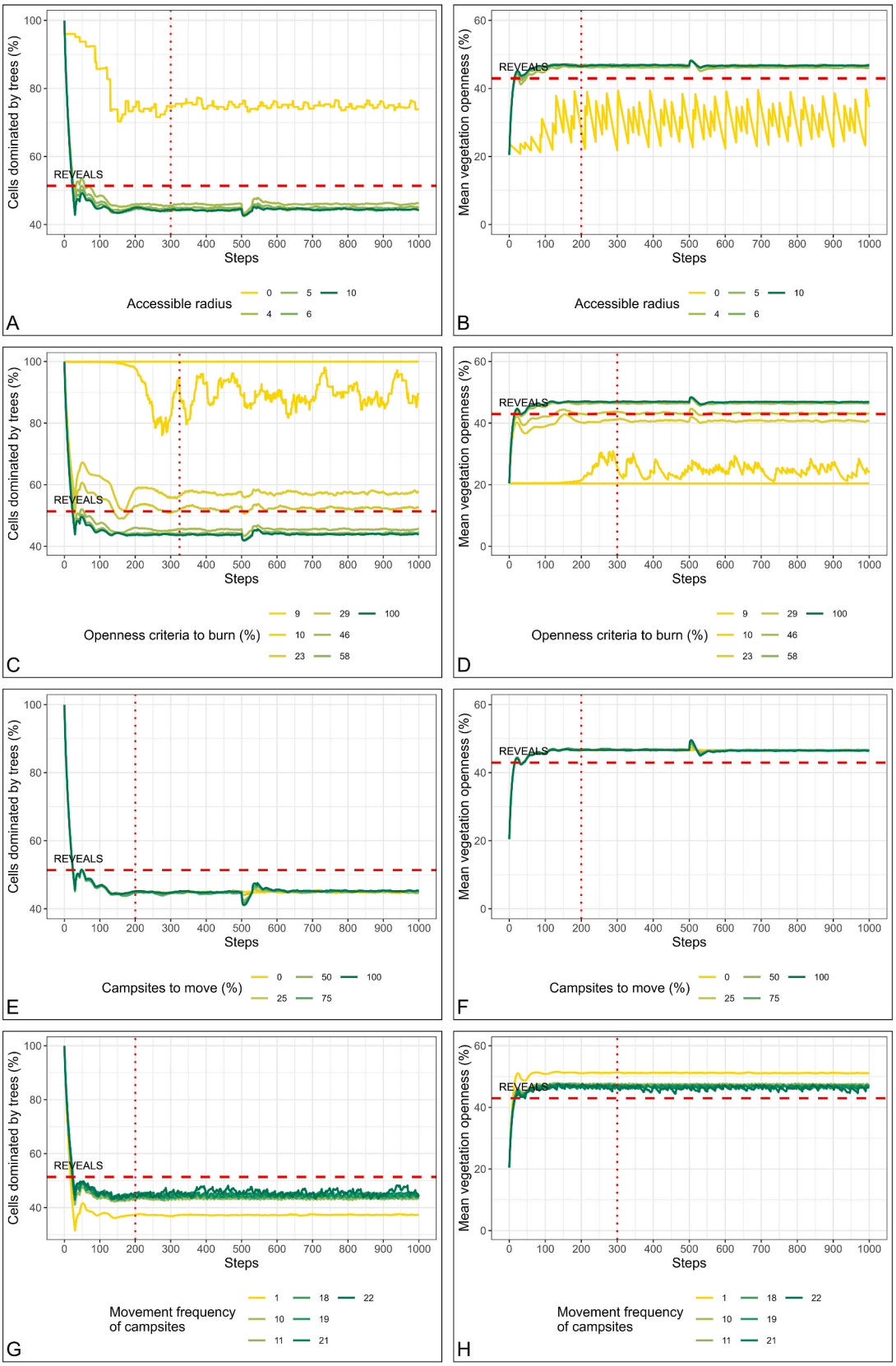

Fig. 6. Results of experiments conducted for 4000 hunter-gatherer groups: A–percentage of grid cells dominated by trees after the accessible radius was varied; B–mean vegetation openness after the accessible radius was varied; C–percentage of cells dominated by trees after the openness criteria to burn was varied; D–mean vegetation openness after the openness criteria to burn was varied; E–percentage of grid cells dominated by trees after the percentage of moving campsites was varied; F–mean vegetation openness after the percentage of moving campsites was varied; G–percentage of grid cells dominated by trees after the movement frequency was varied; H–mean vegetation openness after the movement frequency was varied. Each line depicted on the experiment output graph represents the mean of 30 simulation runs. The horizontal dashed line indicates REVEALS estimates, and the vertical dotted line shows the step when simulations reach equilibrium.

Table 3
Details of the sensitivity analysis experiment.

Parameter	Variable/constant	Min	Max
Territory_impacted_by_thunderstorms	Variable	0.1	7
Megafauna	Constant	True	
Number_of_hunter-gatherer_groups	Variable	1	4000
Accessible_radius	Variable	0	5
Openness_criteria_to_burn	Variable	9	100
Campsites_to_move	Variable	0	100
Movement_frequency_of_campsites	Variable	1	21

assemblages and CARAIB is a dynamic vegetation model driven by climate forcings and assumptions about vegetation dynamics), the observed difference between REVEALS and CARAIB datasets can be partially explained by loss of information due to reclassification and resampling and the difference in the models themselves (Dallmeyer et al., 2023; Zapolska et al., 2023a). Discrepancies between CARAIB and REVEALS can be also partially explained by the different migration vegetation lags in different parts of Europe (e.g., Giesecke et al., 2017; Dallmeyer et al., 2022). However, quantifying the distinctions arising from variations in the models themselves and those resulting from plant migration remains challenging to quantify. The findings of Zapolska et al. (2023b) indicate that incorporating the CDF-t bias correction in the workflow significantly improves the overall reliability of CARAIB results when compared to independent reconstructions. Overall, given the spatio-temporal resolution and aggregated classification (Table 2), despite the acknowledged methodological biases we consider the provided datasets to be sufficiently reliable for the outlined research purposes of this study. CARAIB quantifies the amount of bare ground for each grid cell, unlike REVEALS. Therefore, estimates of bare ground can be used as a potential marker for the comparison results reliability (i.e., high fraction of bare ground indicates low reliability of comparison results) (Fig. S10 with bare ground fraction is available in Appendix A Supplementary data).

Comparing models like REVEALS and CARAIB would require modifying their initial results, as they produce different outputs. To address this issue, HUMLAND uses PFTs (Table 2) to combine CARAIB and REVEALS datasets in a continental-scale ABM. However, this approach may not be suitable for every biogeographical region in Europe, and regional differences between the models are not fully considered in the current study. Moreover, the current study's time constraints are based on REVEALS temporal resolution, which uses 500-year-long time windows to minimize standard errors and study vegetation transformations over millennia (Serge et al., 2023).

It is important to highlight that REVEALS was applied on pollen data from all sites (large lakes>50 ha, and/or multiple sized lakes and bogs). Water bodies such as lakes tend to attract herbivores, and their activity can significantly alter ecosystems by reducing canopy height and structure, increasing in speed dispersal rates and trampling effects, and, therefore, changing plant species competition by promoting grazing-adapted species, transformation of carbon and nutrient cycles, increase in landscape heterogeneity, etc. (Bakker et al., 2016b). Hence, the difference between the REVEALS dataset and the CARAIB reconstruction in terms of higher vegetation openness could be attributed, at least in part, to local pollen counts influenced by the presence of megafauna near the sample sites. However, it is important to note that the vegetation reconstruction derived from REVEALS does not reflect the local conditions immediately around the water bodies where the samples were collected. Instead, it provides a broader perspective of regional and sub-continental vegetation coverage, and has been well validated using modern and historical data (Hellman et al., 2008; Trondman et al., 2016; Marquer et al., 2020). Therefore, the openness values obtained from REVEALS are likely not reflective of only the local impact of herbivores in the vicinity of the lakes.

Thus, it is crucial to emphasize that the CARAIB and REVEALS datasets exhibit substantial dissimilarities. We acknowledge that these disparities stem from factors such as inherent model differences, vegetation migration lags, variable sources of errors, etc. Despite these caveats, it is important to underline that the observed vegetation cover is not solely a product of climatic impact; other factors have also played a pivotal role in shaping vegetation in the study area.

4.2. *What defines the intensity of anthropogenic impact?*

Based on the results of LHS/PRCC, we can conclude that the impact of hunter-gatherer vegetation burning on continental-level is influenced

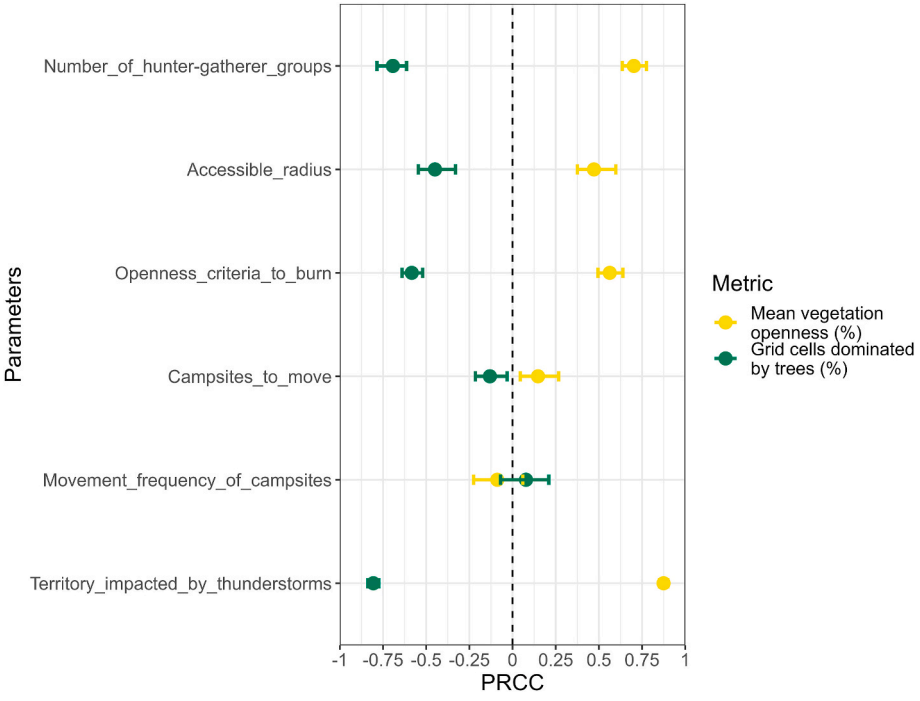

Fig. 7. Results of LHS/PRCC sensitivity analysis with bars representing standard errors.

by three key factors. Firstly, the intensity of these changes is contingent upon the number of hunter-gatherer groups inhabiting a given area, thereby establishing a link between population size and the strength of anthropogenic impact.

Secondly, the extent of human-induced vegetation change is determined by the natural vegetation openness around campsites. This factor might be connected to the preferences of the hunter-gatherers when selecting the location for their campsites. Numerous studies have been conducted on this topic, and among the predominant factors influencing the distribution of campsites are distance to water sources or to coasts, food resources and raw materials availability (e.g., Garcia, 2013; Zolnikov et al., 2013; Abe et al., 2016). The importance of these factors varies depending on the specific study area, period, and subsistence strategies of the hunter-gatherer groups. Other factors, such as surface area roughness or sun exposure, may also play a role (Zolnikov et al., 2013). Vegetation openness can be an additional factor that defines the spatial distribution of hunter-gatherer sites. Depending on the practices of specific hunter-gatherer groups and preferred openness, humans may initially choose naturally open areas that could contain the resources needed. In cases where such areas are not available, hunter-gatherer groups with knowledge of vegetation burning techniques could modify the surrounding environment to match their preferences and make specific areas suitable for their hunting activities and/or (re-)growth of consumed plants. Therefore, the openness of vegetation can be taken into consideration for hunter-gatherers when selecting campsite locations.

The parameters associated with the mobility of hunter-gatherers include Accessible_radius, Campsites_to_move, and Movement_frequency_of_campsites. Among these, Accessible_radius holds a greater influence on the model output compared to the latter two factors, which have minimal contributions to human-induced vegetation changes. This is because these parameters primarily allow the vegetation a chance to recover and return to its natural state in HUMLAND. On the other hand, the accessible radius, with higher values, creates a wider area around campsites that experiences constant anthropogenic impact without sufficient time for recovery. In other words, the movement frequency of campsites and number of campsites that relocate provide opportunities for vegetation to regenerate after anthropogenic impact, allowing these areas to revert to their initial condition. Conversely, a larger accessible radius extends the reach of human influence, creating a broader zone around campsites where vegetation is consistently impacted without adequate time for regrowth.

4.3. First insights into the role of hunter-gatherers and other agents in continental-level vegetation change

There are three types of impact which cause an increase of vegetation openness in this ABM: megafauna plant consumption, natural and human-induced fires. Before addressing the role of humans, it is important to clarify how two other forms of impact reshape the HUMLAND landscapes. While searching for initial potential scenarios to establish a context for human-induced modifications, we maintained parameter values related to the impact of megafauna and natural fires as constants.

The findings of this study reveal that the maximum potential consumption of vegetation by megafauna did not yield significant changes in vegetation (Fig. 4C and D). It is worth considering that our observations might be influenced by the different nature of anthropogenic and megafauna impacts on vegetation. Humans can impact both upper (trees) and lower (shrubs and herbs) levels of vegetation via fire use. In contrast, the influence of megafauna on these vegetation levels depends on the species present in a given area. If large and megaherbivores occupy an area, these animals employ diverse feeding strategies, enabling them to affect vegetation on multiple levels through plant consumption, as well as other forms of impact such as bark stripping and trampling (Beschta et al., 2020; Kowalczyk et al., 2021)–actions that likely reduced the abundance of woody plants (Bakker et al., 2016a; Pedersen et al., 2023). By the time of the Early Holocene, the decline in large animal populations must have lessened their impact on these plants, likely contributing to an increased frequency of fires and the spread of woody vegetation (Bakker et al., 2016a). Our study potentially aligns with this trajectory, as the megafauna impact within the HUMLAND did not diminish the proportion of cells dominated by trees throughout the studied one Early Holocene time window (Fig. 4C).

In HUMLAND simulations, we used estimates of potential maximal megafauna plant consumption. However, this level of consumption may not have been sustained at the same constant intensity level throughout every simulation step, particularly during phases of vegetation recovery after consumption or fires. If megafauna consumption is modelled at every simulation step with the same intensity as in the potential maximal consumption dataset, the HUMLAND output exhibits overestimation of vegetation openness relative to the REVEALS estimates, due to impediment of regrowth of woody vegetation across significant portions of the study area. In light of this, we deliberately excluded the interference of megafauna in the process of vegetation regrowth in HUMLAND. Hence, our modelling is likely to underestimate the effect of megafauna on the vegetation during its regeneration phase after disturbance, as herbivores often seek out such early-successional patches (due to accessibility of forage) and thereby may exert strong influence on tree regeneration (e.g., Kowalczyk et al., 2021). Additionally, the maximal extent of animal plant consumption might have been higher than indicated by the potential maximal megafauna plant consumption dataset due to underestimates of natural densities and overall biomasses caused by anthropogenic pressures across natural areas today (e.g., Robson et al., 2017). Conversely, the HUMLAND model does not incorporate the hunting pressure that humans exerted on these animals and which may have decreased their impact.

Regarding natural fires, achieving the REVEALS estimates solely through the impact of thunderstorms is theoretically possible. However, it would require an unrealistic occurrence of thunderstorms affecting 4.7–7% of the study area every year (Fig. 4A and B), surpassing current estimates of thunderstorm frequency in Europe (see below). Consequently, to align with observed vegetation cover via REVEALS, the inclusion of human influence in our experiments becomes necessary.

To generate preliminary potential scenarios of modified vegetation, the most influential parameters associated with human activities were varied across their minimum, midpoint and maximal round values: Number_of_hunter-gatherer_groups (1, 2001, 4000), Accessible_radius (0, 3, 5), and Openness_criteria_to_burn (9, 55, 100). Campsites_to_move (50) and Movement_frequency_of_campsites (500) remained constant because they are less influential for the model output (sections 3.4 and 4.2).

LHS/PRCC results (Fig. 7) showed that the Territory_impacted_by_thunderstorms parameter has significant impact on the model output, but this parameter was constant during the generation of initial potential scenarios. Due to the absence of continental Early Holocene thunderstorm frequency estimates for Europe, we used decadal lightning observations for Europe during the period of 2008–2017 (Enno et al., 2020). In accordance with these estimates, the majority of Europe experiences 20–40 thunderstorm days per 1 km^2 annually (ibid.). Considering that thunderstorms in HUMLAND can only occur once on a grid cell per simulation step, it would mean that 0.02%–0.04% of all grid cells would encounter the impact of thunderstorms every simulation step. Thus, the Territory_impacted_by_thunderstorms parameter had a constant value of 0.04 during these experiments.

If any variable is set to its minimum value, the model output significantly differs from REVEALS estimates, and they cannot be reached (Fig. 8). All variables should be between their maximal and midpoint values to obtain a scenario which matches REVEALS estimates. Consequently, hunter-gatherers practiced their activities and altered vegetation within a radius of 40–60 km around campsites (equivalent to 3 to 5 grid cells around a cell with a campsite on it in HUMLAND).

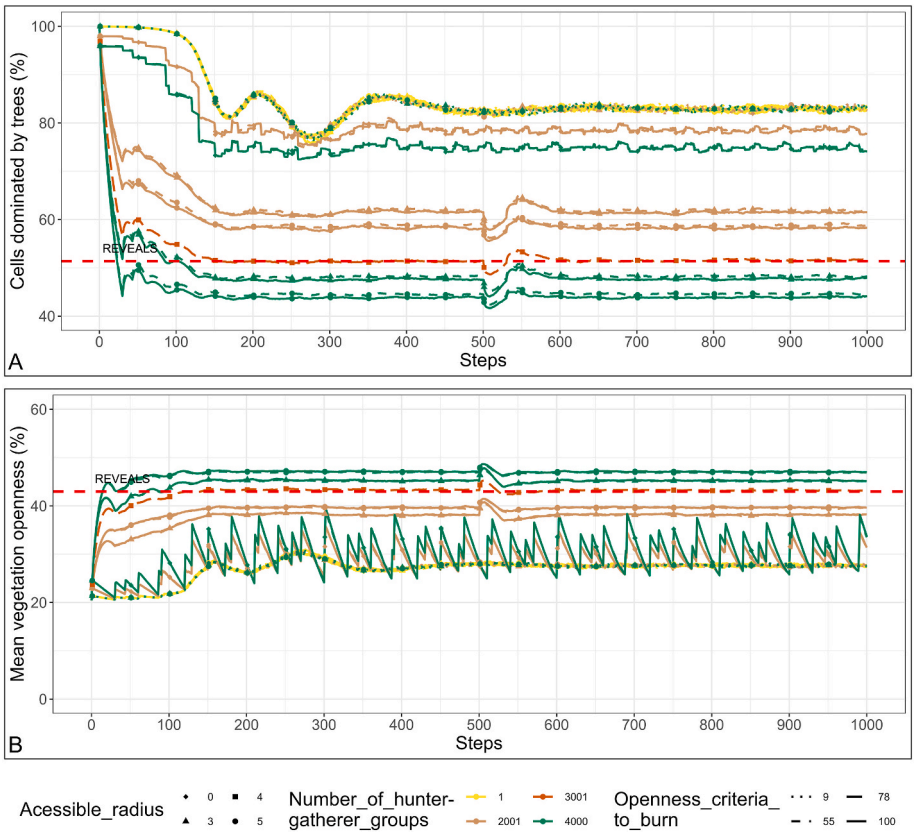

Fig. 8. Percentage of grid cells dominated by trees (A) and mean vegetation openness (B) after combined impact of humans, climate, megafauna and natural fires. The following parameters were varied: number of hunter-gatherer groups, accessible radius and openness criteria to burn. Movement frequency of campsites (500), the number of them which move at specific time (50%), proportion of terrestrial cells with thunderstorms (0.04%) remained constant with fixed presence of megafauna plant consumption. Each line depicted on the experiment output graph represents the mean of 30 simulation runs. The horizontal dashed line indicates REVEALS estimates.

Because the accessible radii in HUMLAND includes both foraging and logistical radii and varies between 0 and 5 grid cells (10–60 km including the grid cell with a campsite on it), the values of this parameter are expected to be more than 0 because this area only includes the foraging radii which is rarely beyond ~10 km (Binford, 1982). Within this range, only plant food, small game and aquatic resources were available for hunter-gatherers. The importance of logistical radii increases with increasing dependence on large games (Kelly, 2013).

Presuming that the assumptions driving our modelling exercise are correct, our results indicate to what extent hunter-gatherer burning of landscapes could explain the landscape openness inferred from REVEALS. It is important to note that preferences for vegetation openness can vary among different hunter-gatherer groups, influenced by their specific adaptations, resource exploitation, and cultural practices. However, our results highlight a general trend of high-frequency human-induced fires. Repetitive small-scale fire use created mosaic environments with a diverse range of resources around their campsites, fostering variability and resource productivity (Scherjon et al., 2015; Bird et al., 2020; Nikulina et al., 2022).

Regarding the population size of hunter-gatherer groups, our results showed that the required number of groups to reach REVEALS estimates falls between 2001 and 4000 groups during the studied period (9200–8700 BP) (Fig. 8). Generally, historically documented hunter-gatherers exhibited significant variation in local group size, with an average of 25 (Kelly, 2013). Given the considerable variability in group size, estimating the population of Mesolithic humans using HUMLAND presents a challenge, and it should be noted that this was not the primary focus of this study. However, based on average estimates of group size, we can suggest that during 9200–8700 BP there were potentially around 50,000–100,000 people at least.

Comparing our estimates with other studies proves challenging due to the variability in already published data regarding hunter-gatherer population size. Some studies indicate that at approximately 13,000 BP, the human population size was estimated to already be around 410,000 individuals (Tallavaara et al., 2015). Conversely, other research suggests that, at 14,700 years BP, the population size was around 155,000 individuals, which then decreased to approximately 143,000 individuals at 11,700 BP (Ordonez and Riede, 2022). The largest population size inferred was around 8000 BP of around 213,900 individuals, with a minimum estimate of around 52,000 individuals and a maximum estimate of approximately 1,111,000 individuals (ibid.). Finally, population size estimated in History database of the Global Environment (HYDE) 3.2. varies between 26,000 and 666,900 during 9000 BP, and between 46,420 and 881,890 during 8000 BP in Europe (Goldewijk et al., 2017). HUMLAND's population estimates are generally lower than other studies showed. This difference arises from HUMLAND's exclusive consideration of fire-utilizing populations, potentially underestimating the overall human population due to the omission of groups which did not practice landscape burning.

The currently obtained results for the three different parameters are still in a preliminary stage. As the first demonstration of the full potential of HUMLAND in identifying the most influential factor in continental-level vegetation change, we have produced one possible scenario which closely aligns with the results obtained through the REVEALS analysis (Fig. 8). In this scenario, we simulated 3001 hunter-gatherer groups that moved and burned areas where the vegetation openness was equal to or lower than 78% within a four-cell radius around their campsites. This scenario matches the REVEALS estimates, as the

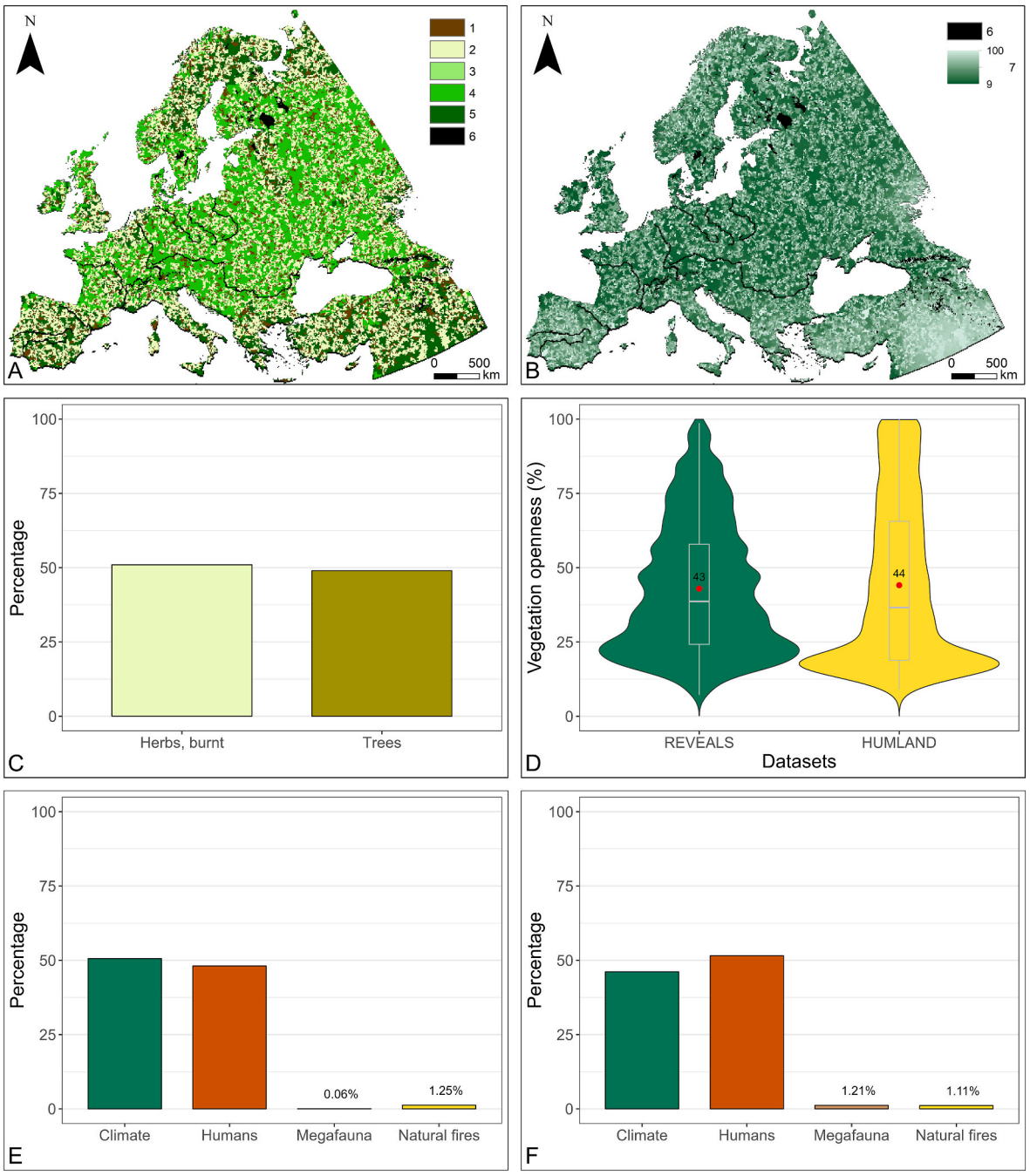

Fig. 9. Possible scenario of modified first dominant PFTs (A), vegetation openness (B), bar graph of dominant PFT proportions (C), summary statistics of vegetation openness and their values' distribution (D; the dot indicates the mean value for each dataset) in the end of a HUMLAND run, and mean percentage of cells modified by different agents (impact on dominant PFTs (E) and vegetation openness (F) during equilibrium state). Dominant PFT proportions and summary statistics of vegetation openness were calculated for the cells with REVEALS and CARAIB estimates after excluding the grid cells where CARAIB predicts lower vegetation openness than the REVEALS results. Legend: 1–recently burnt areas; 2–herbs; 3–shrubs; 4–broadleaf trees; 5–needleleaf trees; 6–no data; 7–vegetation openness in percentages.

averaged ABM output of 30 runs after 450 steps exhibits a similar percentage of trees-dominated cells and mean vegetation openness to the REVEALS results (Fig. 8). The only deviation occurs at step 500 when the human agents relocate their campsites.

The obtained F1-score for this scenario is 0.5 with an accuracy of 0.51. In addition, we conducted a statistical analysis comparing 500 randomly selected grid cells from both the REVEALS and ABM output. The computed t-value was -2 (p-value = 0.03, df = 998). Thus, this scenario has stronger alignment with REVEALS, compared to CARAIB and REVEALS (Figs. 2 and 3). Due to that, this scenario could serve as a possible representation of past modified landscapes (Fig. 9).

Since this scenario matched the REVEALS data, we further examined the extent of modifications performed by each agent. Specifically, we averaged the observations of the number of grid cells modified by each agent from steps 450 to 1000 (Fig. 9E and F). Climate and humans were estimated as the factors responsible for the majority of changes, whereas megafauna and natural fires caused by thunderstorms in this ABM played a smaller role as evidenced by the mean number of grid cells modified by each agent during the equilibrium state. These findings suggest that humans and climate were the most influential factors in

driving continental-level vegetation changes, while natural fires and megafauna activities in HUMLAND had less impact.

Increased burning during the Early Holocene has been previously identified in Europe on the basis of sedimentary charcoal records (Marlon et al., 2013). It was suggested that the impact of anthropogenic fire use was limited, mainly due to the relatively low population size (ibid.). High fire activity aligned with ecosystems reorganization as a result of deglaciation (ibid.). Our results suggest that early anthropogenic impact on the environment was the principal non-climate factor affecting landscapes during the early Holocene, in line with evidence obtained in other parts of the world (Ellis et al., 2021). It is important to highlight that our observations represent general patterns at the continental level. We acknowledge the possibility of regional variations, i.e., instances where humans may have had a smaller impact compared to climate, megafauna, and natural fires, and we also note the limitations to representation of some of these factors in the model.

5. Conclusion

We introduced the novel HUMLAND ABM application, capable of tracking and quantifying different types of impact on interglacial vegetation at the continental level. We compared the climate-based (CARAIB) and pollen reconstruction-based (REVEALS) estimates for vegetation cover for a specific time window (9200–8700 BP), and our findings show a substantial disparity between the two datasets. We conclude that climate is just one of several factors contributing to the observed vegetation patterns, and other drivers also played an important role.

Our analysis showed that humans could constitute the primary non-climate drivers shaping European landscapes in the period analysed. The extent of anthropogenic vegetation modifications hinges primarily on three key parameters: the number of human groups, vegetation openness around campsites, and the size of an area impacted by humans. The first obtained scenario emphasized that humans had a strong impact on vegetation during the Early Holocene.

This study highlights the feasibility of creating a modelling approach suitable for tracking and quantifying the intensity of different impacts on interglacial landscapes at the continental level. Future work can focus on increasing the number of time steps to mitigate the differences between REVEALS and CARAIB datasets, and thus enhance our understanding of past processes by examining the temporal progression of our modelling exercises and their findings. In addition, more work is needed on how to represent the role of megafauna in vegetation dynamics and the potential role of hunting and other human activities therein.

Overall, this research contributes to our understanding of past human-environment interactions and demonstrates the potential of the HUMLAND ABM. The identified challenges and future directions highlight the need for continued interdisciplinary efforts and the acquisition of high-quality datasets to refine and expand the capabilities of ABM-based studies in studying anthropogenic impacts on landscapes.

CRediT authorship contribution statement

Anastasia Nikulina: Conceptualization, Methodology, Software, Validation, Formal analysis, Investigation, Data curation, Writing - original draft, Visualization, Project administration. **Katharine MacDonald:** Conceptualization, Methodology, Resources, Supervision. **Anhelina Zapolska:** Methodology, Investigation, Resources, Writing - original draft. **Maria Antonia Serge:** Methodology, Investigation, Resources, Writing - original draft. **Didier M. Roche:** Methodology, Resources, Writing - review & editing, Supervision. **Florence Mazier:** Methodology, Resources, Writing - review & editing, Supervision. **Marco Davoli:** Methodology, Investigation, Resources, Writing - original draft. **Jens-Christian Svenning:** Methodology, Resources, Writing - review & editing, Supervision. **Dave van Wees:** Investigation, Resources, Writing - original draft. **Elena A. Pearce:** Methodology, Writing - review & editing. **Ralph Fyfe:** Methodology, Resources, Writing - review & editing, Supervision. **Wil Roebroeks:** Conceptualization, Methodology, Resources, Writing - review & editing, Supervision, Project administration. **Fulco Scherjon:** Conceptualization, Methodology, Software, Validation, Resources, Writing - review & editing, Supervision, Project administration.

Declaration of competing interest

The authors declare that they have no known competing financial interests or personal relationships that could have appeared to influence the work reported in this paper.

Data availability

HUMLAND ABM is available via the CoMSES library (https://doi.org/10.25937/fxdq-fn86). The simulation results and the R project have been uploaded to the Zenodo repository (https://doi.org/10.5281/zenodo.10006039).

Acknowledgments

The research is financed through the European Union's Horizon 2020 research and innovation programme within the TERRANOVA project, No 813904, and supported by the Liveable Planet programme of Leiden University. The paper reflects the views only of the authors, and the European Union cannot be held responsible for any use which may be made of the information contained therein. Jens-Christian Svenning was further supported by the VILLUM Investigator project "Biodiversity Dynamics in a Changing World", funded by VILLUM FONDEN (grant 16549), Center for Ecological Dynamics in a Novel Biosphere (ECONOVO), funded by Danish National Research Foundation (grant DNRF173), and the Independent Research Fund Denmark Natural Sciences project MegaComplexity (grant 0135–00225B). This work was performed using compute resources from the Academic Leiden Interdisciplinary Cluster Environment (ALICE) provided by Leiden University. We would like to thank Prof. Jan Kolen (Leiden University, The Netherlands), Prof. Corrie Bakels (Leiden University, The Netherlands), Prof. Marie-Jose Gaillard-Lemdahl (Linnaeus University, Sweden), Dr. Tuna Kalayci (Leiden University, The Netherlands), Frank Arthur (University College of Southeast Norway, Norway), Prof. Hans Renssen (University College of Southeast Norway, Norway), Dr. Izabella Romanowska (Aarhus University, Denmark), Dr. Alex Brandsen (Leiden University, The Netherlands), Dr. Gabriela Florescu (Stefan cel Mare University, Suceava, Romania), Dr. Kim Cohen (Utrecht University, The Netherlands), Cyril Piou (CIRAD, France), Dr. Anneli Poska (Lund University, Sweden; Tallinn University of Technology, Estonia), Dr. Dennis Braekmans (Leiden University, The Netherlands), Dr. Lucile Marescot (CIRAD, France), Agnes Schneider (Leiden University, The Netherlands), Femke Reidsma (Leiden University, The Netherlands), Dr. Andrew Sorensen (Leiden University, The Netherlands), Prof. Guido R. van der Werf (Vrije University, The Netherlands), Dr. Nicolas Viovy (Université Paris-Saclay, France), Julian Coupas (France), Dr. Wouter Verschoof-van der Vaart (Leiden University, The Netherlands), and Bjørn Peare Bartholdy (Leiden University, The Netherlands). We extend our gratitude to all the members of the Human Origins group at Leiden University (The Netherlands). The authors would also like to thank Prof. Louis M. François (University of Liège, Belgium) for providing the CARAIB global dynamic vegetation model and his help in running it.

Appendix A. Supplementary data

Supplementary data to this article can be found online at https://doi.org/10.1016/j.quascirev.2023.108439.

References

Abe, C., Leipe, C., Tarasov, P.E., Müller, S., Wagner, M., 2016. Spatio-temporal distribution of hunter–gatherer archaeological sites in the Hokkaido region (northern Japan): an overview. Holocene 26 (10), 1627–1645. https://doi.org/10.1177/0959683616641745.

Archibald, S., Lehmann, C.E.R., Gómez-Dans, J.L., Bradstock, R.A., 2013. Defining pyromes and global syndromes of fire regimes. Proc. Natl. Acad. Sci. U.S.A. 110 (16), 6442–6447. https://doi.org/10.1073/pnas.1211466110.

Arthur, F., Roche, D.M., Fyfe, R., Quiquet, A., Renssen, H., 2023. Simulations of the Holocene climate in Europe using an interactive downscaling within the iLOVECLIM model (version 1.1). Clim. Past 19 (1), 87–106. https://doi.org/10.5194/cp-19-87-2023.

Bakker, E.S., Gill, J.L., Johnson, C.N., Vera, F.W.M., Sandom, C.J., Asner, G.P., Svenning, J.-C., 2016a. Combining paleo-data and modern exclosure experiments to assess the impact of megafauna extinctions on woody vegetation. Proc. Natl. Acad. Sci. U.S.A. 113 (4), 847–855. https://doi.org/10.1073/pnas.1502545112.

Bakker, E.S., Pagès, J.F., Arthur, R., Alcoverro, T., 2016b. Assessing the role of large herbivores in the structuring and functioning of freshwater and marine angiosperm ecosystems. Ecography 39 (2), 162–179. https://doi.org/10.1111/ecog.01651.

Beschta, R.L., Ripple, W.J., Kauffman, J.B., Painter, L.E., 2020. Bison limit ecosystem recovery in northern Yellowstone. Food Webs 23. https://doi.org/10.1016/j.fooweb.2020.e00142.

Binford, L.R., 1982. The archaeology of place. J. Anthropol. Archaeol. 1 (1), 5–31. https://doi.org/10.1016/0278-4165(82)90006-X.

Bird, R.B., McGuire, C., Bird, D.W., Price, M.H., Zeanah, D., Nimmo, D.G., 2020. Fire mosaics and habitat choice in nomadic foragers. Proc. Natl. Acad. Sci. U.S.A. 117 (23), 12904–12914. https://doi.org/10.1073/pnas.1921709117.

Bistinas, I., Oom, D., Sá, A.C.L., Harrison, S.P., Prentice, I.C., Pereira, J.M.C., 2013. Relationships between human population density and burned area at continental and global scales. PLoS One 8 (12), 1–12. https://doi.org/10.1371/journal.pone.0081188.

Bond, W.J., Wilgen, B. W. van, 1996. Fire and Plants. Chapman & Hall.

Boogers, S., Daems, D., 2022. SAGAscape: simulating resource exploitation strategies in iron age to hellenistic communities in southwest Anatolia. J. Comput. Appl. Archaeol. 5 (1), 169. https://doi.org/10.5334/jcaa.90.

Bos, J.A.A., Urz, R., 2003. Late Glacial and early Holocene environment in the middle Lahn river valley (Hessen, central-west Germany) and the local impact of early Mesolithic people—pollen and macrofossil evidence. Veg. Hist. Archaeobotany 12, 19–36. https://doi.org/10.1007/s00334-003-0006-7.

Cao, X., Tian, F., Li, F., Gaillard, M.J., Rudaya, N., Xu, Q., Herzschuh, U., 2019. Pollen-based quantitative land-cover reconstruction for northern Asia covering the last 40 ka cal BP. Clim. Past 15 (4). https://doi.org/10.5194/cp-15-1503-2019.

Caseldine, C., Hatton, J., 1993. The development of high moorland on Dartmoor: fire and the influence of Mesolithic activity on vegetation change. Clim. Chang. Human Impact Landsc. 119–131. https://doi.org/10.1007/978-94-011-2292-4_14.

Ch'ng, E., Gaffney, V.L., 2013. Simulation and visualisation of agent survival and settlement behaviours in the hunter-gatherer colonisation of mesolithic landscapes. In: Ch'ng, H., Eugene, Gaffney, Vincent, Chapman (Eds.), Visual Heritage in the Digital Age. Springer-Verlag, pp. 235–258. http://www.springer.com/series/10481.

Crees, J.J., Collen, B., Turvey, S.T., 2019. Bias, incompleteness and the "known unknowns" in the Holocene faunal record. Phil. Trans. Biol. Sci. 374 (1788) https://doi.org/10.1098/rstb.2019.0216.

Dallmeyer, A., Kleinen, T., Claussen, M., Weitzel, N., Cao, X., Herzschuh, U., 2022. The deglacial forest conundrum. Nat. Commun. 13 (1), 1–10. https://doi.org/10.1038/s41467-022-33646-6.

Dallmeyer, A., Poska, A., Marquer, L., Seim, A., Gaillard-Lemdahl, M.-J., 2023. The challenge of comparing pollen-based quantitative vegetation reconstructions with outputs from vegetation models – a European perspective. Clim. Past Discuss 1–50. https://cp.copernicus.org/preprints/cp-2023-16/.

Danielson, J.J., Gesch, D.B., 2011. Global Multi-Resolution Terrain Elevation Data 2010 (GMTED2010). *Open-File Report*. https://doi.org/10.3133/ofr20111073.

Davies, P., Robb, J.G.R., Ladbrook, D., 2005. Woodland clearance in the Mesolithic: the social aspects. Antiquity 79, 280–288.

Université de Liège. (n.d.). Caraib. http://www.umccb.ulg.ac.be/Sci/m_car_e.html.

Davoli, M., Monsarrat, S., Pedersen, R., Scussolini, P., Karger, D.N., Normand, S., Svenning, J.-C., 2023. Megafauna diversity and functional declines in Europe from the Last Interglacial to the present. Global Ecology and Biogeography 00 (1–14). https://doi.org/10.1111/geb.13778.

Dennis, F.C., 1999. Fire-resistant landscaping. Nat. Resour. Ser. Forestry 6, 303.

Dietze, E., Theuerkauf, M., Bloom, K., Brauer, A., Dörfler, W., Feeser, I., Feurdean, A., Gedminiene, L., Giesecke, T., Jahns, S., Karpińska-Kołaczek, M., Kołaczek, P., Lamentowicz, M., Latałowa, M., Marcisz, K., Obremska, M., Pędziszewska, A., Poska, A., Rehfeld, K., et al., 2018. Holocene fire activity during low-natural flammability periods reveals scale-dependent cultural human-fire relationships in Europe. Quat. Sci. Rev. 201, 44–56. https://doi.org/10.1016/j.quascirev.2018.10.005.

Doran, J.D., Randall, C.K., Long, A.J., 2004. Fire in the Wildland-Urban Interface: Selecting and Maintaining Firewise Plants for Landscaping. University of Florida; USDA Forest Service. https://doi.org/10.32473/edis-fr147-2004.

Dury, M., Hambuckers, A., Warnant, P., Henrot, A., Favre, E., Ouberdous, M., François, L., 2011. Responses of European forest ecosystems to 21st century climate: assessing changes in interannual variability and fire intensity. IForest 4, 82–99. https://doi.org/10.3832/ifor0572-004.

Ellis, E., Maslin, M., Boivin, N., Bauer, A., 2016. Involve social scientists in defining the Anthropocene. Nature 540, 192–193. https://doi.org/10.1038/540192a.

Ellis, E.C., Gauthier, N., Goldewijk, K.K., Bird, R.B., Boivin, N., Díaz, S., Fuller, D.Q., Gill, J.L., Kaplan, J.O., Kingston, N., Locke, H., McMichael, C.N.H., Ranco, D., Rick, T.C., Rebecca Shaw, M., Stephens, L., Svenning, J.C., Watson, J.E.M., 2021. People have shaped most of terrestrial nature for at least 12,000 years. Proc. Natl. Acad. Sci. U.S.A. 118 (17), 1–8. https://doi.org/10.1073/pnas.2023483118.

Ember, C.R., 2020. Hunter-gatherers. Explaining human culture. Human relations area files. https://hraf.yale.edu/ehc/summaries/hunter-gatherers.

Enno, S.E., Sugier, J., Alber, R., Seltzer, M., 2020. Lightning flash density in Europe based on 10 years of ATDnet data. Atmos. Res. 235, 104769 https://doi.org/10.1016/j.atmosres.2019.104769.

European Commission. (n.d.). Water information system for Europe (WISE). https://water.europa.eu/.

Faurby, S., Svenning, J.C., 2015. Historic and prehistoric human-driven extinctions have reshaped global mammal diversity patterns. Divers. Distrib. 21 (10), 1155–1166. https://doi.org/10.1111/ddi.12369.

Feurdean, A., Liakka, J., Vannière, B., Marinova, E., Hutchinson, S.M., Mosburgger, V., Hickler, T., 2013. 12,000-Years of fire regime drivers in the lowlands of Transylvania (Central-Eastern Europe): a data-model approach. Quat. Sci. Rev. 81 (1), 48–61.

Feurdean, A., Veski, S., Florescu, G., Vannière, B., Pfeiffer, M., O'Hara, R.B., Stivrins, N., Amon, L., Heinsalu, A., Vassiljev, J., Hickler, T., 2017. Broadleaf deciduous forest counterbalanced the direct effect of climate on Holocene fire regime in hemiboreal/boreal region (NE Europe). Quat. Sci. Rev. 169, 378–390. https://doi.org/10.1016/j.quascirev.2017.05.024.

Feurdean, A., Tonkov, S., Pfeiffer, M., Panait, A., Warren, D., Vannière, B., Marinova, E., 2019. Fire frequency and intensity associated with functional traits of dominant forest type in the Balkans during the Holocene. Eur. J. For. Res. 138 (6), 1049–1066. https://doi.org/10.1007/s10342-019-01223-0.

François, L., Utescher, T., Favre, E., Henrot, A.J., Warnant, P., Micheels, A., Erdei, B., Suc, J.P., Cheddadi, R., Mosbrugger, V., 2011. Modelling Late Miocene vegetation in Europe: results of the CARAIB model and comparison with palaeovegetation data. Palaeogeogr. Palaeoclimatol. Palaeoecol. 304 (3–4), 359–378. https://doi.org/10.1016/j.palaeo.2011.01.012.

Friedl, M., Sulla-Menashe, D., 2019. MCD12Q1 MODIS/Terra+Aqua Land Cover Type Yearly L3 Global 500m SIN Grid V006, NASA EOSDIS L. Process. DAAC. https://doi.org/10.5067/MODIS/MCD12Q1.006.

Garcia, A., 2013. GIS-based methodology for Palaeolithic site location preferences analysis. A case study from Late Palaeolithic Cantabria (Northern Iberian Peninsula). J. Archaeol. Sci. 40 (1), 217–226. https://doi.org/10.1016/j.jas.2012.08.023.

Gesch, D.B., Verdin, K.L., Greenlee, S.K., 1999. New land surface digital elevation model covers the earth. Eos 80 (6), 69–70. https://doi.org/10.1029/99EO00050.

Giesecke, T., Brewer, S., Finsinger, W., Leydet, M., Bradshaw, R.H.W., 2017. Patterns and dynamics of European vegetation change over the last 15,000 years. J. Biogeogr. 44 (7), 1441–1456. https://doi.org/10.1111/jbi.12974.

Giglio, L., Boschetti, L., Roy, D.P., Humber, M.L., Justice, C.O., 2018. The Collection 6 MODIS burned area mapping algorithm and product. Rem. Sens. Environ. 217, 72–85. https://doi.org/10.1016/j.rse.2018.08.005.

Githumbi, E., Fyfe, R., Gaillard, M., Trondman, A., Mazier, F., 2022. European pollen-based REVEALS land-cover reconstructions for the Holocene: methodology, mapping and potentials. Earth Syst. Sci. Data 14 (4), 1581–1619.

Goldewijk, K.K., Beusen, A., Doelman, J., Stehfest, E., 2017. Anthropogenic land use estimates for the Holocene - HYDE 3.2. Earth Syst. Sci. Data 9 (2), 927–953. https://doi.org/10.5194/essd-9-927-2017.

Goosse, H., Brovkin, V., Fichefet, T., Haarsma, R., Huybrechts, P., Jongma, J., Mouchet, A., Selten, F., Barriat, P.Y., Campin, J.M., Deleersnijder, E., Driesschaert, E., Goelzer, H., Janssens, I., Loutre, M.F., Morales Maqueda, M.A., Opsteegh, T., Mathieu, P.P., Munhoven, G., et al., 2010. Description of the Earth system model of intermediate complexity LOVECLIM version 1.2. Geosci. Model Dev. (GMD) 3 (2), 603–633. https://doi.org/10.5194/gmd-3-603-2010.

Gowlett, J.A.J., Wrangham, R.W., 2013. Earliest fire in Africa: towards the convergence of archaeological evidence and the cooking hypothesis. Azania 48 (1), 5–30. https://doi.org/10.1080/0067270X.2012.756754.

Gronenborn, D., Horejs, B., 2021. Expansion of Farming in Western Eurasia, 9600 - 4000 Cal BC (Update Vers. 2021.2), vol. 2021. Zenodo, p. 2. https://doi.org/10.5281/zenodo.5903165.

Gumiński, W., Michniewicz, M., 2003. Forest and mobility. A case from the fishing camp dudka, masuria, north-eastern Poland. In: Larsson, L. (Ed.), Mesolithic on the Move. Papers Presented at the Sixth International Conference on the Mesolithic in Europe. Oxbow Books, pp. 119–127.

Hamby, D.M., 1994. A review of techniques for parameter sensitivity. Environ. Monit. Assess. 32, 135–154.

Hamon, C., Manen, C., 2021. The mechanisms of neolithisation of western Europe: beyond a south/north approach. Open Archaeol. 7 (1), 718–735. https://doi.org/10.1515/opar-2020-0164.

Harrison, S.P., Prentice, I.C., Bloomfield, K.J., Dong, N., Forkel, M., Forrest, M., Ningthoujam, R.K., Pellegrini, A., Shen, Y., Baudena, M., Cardoso, A.W., Huss, J.C., Joshi, J., Oliveras, I., Pausas, J.G., Simpson, K.J., 2021. Understanding and modelling wildfire regimes: an ecological perspective. Environ. Res. Lett. 16 (12) https://doi.org/10.1088/1748-9326/ac39be.

Heidgen, S., Marinova, E., Nelle, O., Ebner, M., Rotava, T., Tafelmaier, Y., Krauß, R., Bofinger, J., Junginger, A., 2022. Palaeoecological signals for Mesolithic land use in a Central European landscape? J. Quat. Sci. 37 (6), 1164–1179. https://doi.org/10.1002/jqs.3422.

Hellman, S.E.V., Gaillard, M.J., Broström, A., Sugita, S., 2008. Effects of the sampling design and selection of parameter values on pollen-based quantitative reconstructions of regional vegetation: a case study in southern Sweden using the

REVEALS model. Veg. Hist. Archaeobotany 17 (5), 445–459. https://doi.org/10.1007/s00334-008-0149-7.
Henrot, A.J., Utescher, T., Erdei, B., Dury, M., Hamon, N., Ramstein, G., Krapp, M., Herold, N., Goldner, A., Favre, E., Munhoven, G., François, L., 2017. Middle Miocene climate and vegetation models and their validation with proxy data. Palaeogeogr. Palaeoclimatol. Palaeoecol. 467, 95–119. https://doi.org/10.1016/j.palaeo.2016.05.026.
Hjelle, K.L., Lødøen, T.K., 2017. Dating of rock art and the effect of human activity on vegetation: the complementary use of archaeological and scientific methods. Quat. Sci. Rev. 168, 194–207. https://doi.org/10.1016/j.quascirev.2017.05.003.
Hörnberg, G., Bohlin, E., Hellberg, E., Bergman, I., Zackrisson, O., Olofsson, A., Wallin, J.-E., Påsse, T., 2006. Effects of Mesolithic hunter-gatherers on local vegetation in a non-uniform glacio-isostatic land uplift area, northern Sweden. Veg. Hist. Archaeobotany 15 (1), 13–26. https://doi.org/10.1007/s00334-005-0006-x.
Hunt, C.O., Gilbertson, D.D., Rushworth, G., 2012. A 50,000-year record of late Pleistocene tropical vegetation and human impact in lowland Borneo. Quat. Sci. Rev. 37, 61–80. https://doi.org/10.1016/j.quascirev.2012.01.014.
Iman, R.L., Conover, W.J., 1980. Small sample sensitivity analysis techniques for computer models, with an application to risk assessment. Commun. Stat. Theor. Methods 9 (17), 1749–1842. https://doi.org/10.1080/03610928008827996.
Innes, J.B., Blackford, J.J., Rowley-Conwy, P.A., 2013. Late Mesolithic and early Neolithic forest disturbance: a high resolution palaeoecological test of human impact hypotheses. Quat. Sci. Rev. 77, 80–100. https://doi.org/10.1016/j.quascirev.2013.07.012.
Johnson, E.A., Miyanishi, K., 2021. Disturbance and succession. In: Johnson, E.A., Miyanishi, K. (Eds.), Plant Disturbance Ecology, second ed. Academic Press.
Kaal, J., Criado-Boado, F., Costa-Casais, M., López-Sáez, J.A., López-Merino, L., Mighall, T., Carrión, Y., Silva Sánchez, N., Martínez Cortizas, A., 2013. Prehistoric land use at an archaeological hot-spot (the rock art park of Campo Lameiro, NW Spain) inferred from charcoal, synanthropic pollen and non-pollen palynomorph proxies. J. Archaeol. Sci. 40 (3), 1518–1527. https://doi.org/10.1016/j.jas.2012.09.024.
Kaplan, J.O., Pfeiffer, M., Kolen, J.C.A., Davis, B.A.S., 2016. Large scale anthropogenic reduction of forest cover in last glacial maximum Europe. PLoS One 11 (11), 1–17. https://doi.org/10.1371/journal.pone.0166726.
Kelly, R.L., 2013. The Lifeways of Hunter-Gatherers: the Foraging Spectrum. Cambridge University Press.
Kleynhans, E.J., Atchley, A.L., Michaletz, S.T., 2020. Modeling fire effects on plants: from organs to ecosystems. In: Johnson, E.A., Miyanishi, K. (Eds.), Plant Disturbance Ecology, second ed. Academic Press, pp. 383–421. https://doi.org/10.1016/B978-0-12-818813-2.00011-3.
Knorr, W., Kaminski, T., Arneth, A., Weber, U., 2014. Impact of human population density on fire frequency at the global scale. Biogeosciences 11 (4), 1085–1102. https://doi.org/10.5194/bg-11-1085-2014.
Kowalczyk, R., Kamiński, T., Borowik, T., 2021. Do large herbivores maintain open habitats in temperate forests? For. Ecol. Manag. 494 https://doi.org/10.1016/j.foreco.2021.119310.
Kuhn, M., 2008. Building predictive models in R using the caret package. J. Stat. Software 28, 1–26. https://doi.org/10.18637/jss.v028.i05.
Lake, M.W., 2000. MAGICAL computer simulation of mesolithic foraging. In: Kohler, G.J. G.Timothy A. (Ed.), Dynamics in Human and Primate Societies: Agent-Based Modeling of Social and Spatial Processes. Oxford University Press, pp. 107–144. https://doi.org/10.1093/oso/9780195131673.003.0011.
Lange, S., 2019. EartH2Observe, WFDEI and ERA-interim data merged and bias-corrected for ISIMIP (EWEMBI). V. 1.1. GFZ data services. https://doi.org/10.5880/pik.2019.004.
Laurent, J.M., François, L., Bar-Hen, A., Bel, L., Cheddadi, R., 2008. European bioclimatic affinity groups: data-model comparisons. Global Planet. Change 61 (1–2), 28–40. https://doi.org/10.1016/j.gloplacha.2007.08.017.
Li, F., Gaillard, M.J., Cao, X., Herzschuh, U., Sugita, S., Ni, J., Zhao, Y., An, C., Huang, X., Li, Y., Liu, H., Sun, A., Yao, Y., 2023. Gridded pollen-based Holocene regional plant cover in temperate and northern subtropical China suitable for climate modelling. Earth Syst. Sci. Data 15 (1), 95–112. https://doi.org/10.5194/essd-15-95-2023.
Marino, S., Hogue, I.B., Ray, C.J., Kirschner, D.E., 2008. A methodology for performing global uncertainty and sensitivity analysis in systems biology. J. Theor. Biol. 254 (1), 178–196. https://doi.org/10.1016/j.jtbi.2008.04.011.
Marlon, J.R., Bartlein, P.J., Daniau, A.L., Harrison, S.P., Maezumi, S.Y., Power, M.J., Tinner, W., Vanniére, B., 2013. Global biomass burning: a synthesis and review of Holocene paleofire records and their controls. Quat. Sci. Rev. 65, 5–25. https://doi.org/10.1016/j.quascirev.2012.11.029.
Marquer, L., Gaillard, M.J., Sugita, S., Poska, A., Trondman, A.K., Mazier, F., Nielsen, A. B., Fyfe, R.M., Jönsson, A.M., Smith, B., Kaplan, J.O., Alenius, T., Birks, H.J.B., Bjune, A.E., Christiansen, J., Dodson, J., Edwards, K.J., Giesecke, T., Herzschuh, U., et al., 2017. Quantifying the effects of land use and climate on Holocene vegetation in Europe. Quat. Sci. Rev. 171, 20–37. https://doi.org/10.1016/j.quascirev.2017.07.001.
Marquer, L., Mazier, F., Sugita, S., Galop, D., Houet, T., Faure, E., Gaillard, M.J., Haunold, S., de Munnik, N., Simonneau, A., De Vleeschouwer, F., Le Roux, G., 2020. Pollen-based reconstruction of Holocene land-cover in mountain regions: evaluation of the landscape reconstruction algorithm in the vicdessos valley, northern pyrenees, France. Quat. Sci. Rev. 228 https://doi.org/10.1016/j.quascirev.2019.106049.
Mason, S.L.R., 2000. Fire and Mesolithic subsistence - managing oaks for acorns in northwest Europe? Palaeogeogr. Palaeoclimatol. Palaeoecol. 164 (1–4), 139–150. https://doi.org/10.1016/S0031-0182(00)00181-4.
Mazier, F., Gaillard, M.J., Kuneš, P., Sugita, S., Trondman, A.K., Broström, A., 2012. Testing the effect of site selection and parameter setting on REVEALS-model estimates of plant abundance using the Czech Quaternary Palynological Database. Rev. Palaeobot. Palynol. 187, 38–49. https://doi.org/10.1016/j.revpalbo.2012.07.017.
McKay, M.D., Beckman, R.J., Conover, W.J., 1979. A comparison of three methods for selecting values of input variables in the analysis of output from a computer code. Technometrics 21 (2), 239–245. https://doi.org/10.1080/00401706.2000.10485979.
Mellars, P., 1976. Fire ecology, Animal Populations and Man: a Study of some Ecological Relationships in Prehistory. Proceedings of the Prehistoric Society 42, 15–45. https://doi.org/10.1017/S0079497X00010689.
Mellars, P., Dark, P. (Eds.), 1998. Star Carr in Context: New Archaeological and Palaeoecolgical Investigations at the Early Mesolithic Site of Star Carr. McDonald Institute Monographs, North Yorkshire.
Milisauskas, S., 2002. Early neolithic, the first farmers in Europe, 7000-5500/5000 BC. In: Milisauskas, S. (Ed.), European Prehistory. Springer Science, Business Media, pp. 143–192.
Milner, N., Conneller, C., Taylor, B., 2018. Star Carr: A Persistent Place in a Changing World, vol. 1. White Rose University Press.
Newman, E.A., Kennedy, M.C., Falk, D.A., McKenzie, D., 2019. Scaling and complexity in landscape ecology. Front. Ecol. Evol. 7 https://doi.org/10.3389/fevo.2019.00293.
Nikulina, A., MacDonald, K., Scherjon, F., A, Pearce, E., Davoli, M., Svenning, J.C., Vella, E., Gaillard, M.J., Zapolska, A., Arthur, F., Martinez, A., Hatlestad, K., Mazier, F., Serge, M.A., Lindholm, K.J., Fyfe, R., Renssen, H., Roche, D.M., Kluiving, S., Roebroeks, W., 2022. Tracking hunter-gatherer impact on vegetation in last interglacial and Holocene Europe: proxies and challenges. In: Journal of Archaeological Method and Theory. https://doi.org/10.1007/s10816-021-09546-2.
Novenko, E.Y., Tsyganov, A.N., Payne, R.J., Mazei, N.G., Volkova, E.M., Chernyshov, V. A., Kupriyanov, D.A., Mazei, Y.A., 2018. Vegetation dynamics and fire history at the southern boundary of the forest vegetation zone in European Russia during the middle and late Holocene. Holocene 28 (2), 308–322. https://doi.org/10.1177/0959683617721331.
Ordonez, A., Riede, F., 2022. Changes in limiting factors for forager population dynamics in Europe across the last glacial-interglacial transition. Nat. Commun. 13 (1) https://doi.org/10.1038/s41467-022-32750-x.
Otto, D., Rasse, D., Kaplan, J., Warnant, P., François, L., 2002. Biospheric carbon stocks reconstructed at the Last Glacial Maximum: comparison between general circulation models using prescribed and computed sea surface temperatures. Global Planet. Change 33 (1–2), 117–138. https://doi.org/10.1016/S0921-8181(02)00066-8.
Pedersen, R.Ø., Faurby, S., Svenning, J., 2023. Late-Quaternary megafauna extinctions have strongly reduced mammalian vegetation consumption. Global Ecol. Biogeogr. 1–13. https://doi.org/10.1111/geb.13723. October 2022.
Pinter, N., Fiedel, S., Keeley, J.E., 2011. Fire and vegetation shifts in the Americas at the vanguard of Paleoindian migration. Quat. Sci. Rev. 30 (3–4), 269–272. https://doi.org/10.1016/j.quascirev.2010.12.010.
Pitkänen, A., Tolonen, K., Jungner, H., 2001. A basin-based approach to the long-term history of forest fires as determined from peat strata. Holocene 11 (5), 599–605. https://doi.org/10.1191/095968301680223558.
Popova, S., Utescher, T., Gromyko, D.V., Mosbrugger, V., Herzog, E., François, L., 2013. Vegetation change in Siberia and the northeast of Russia during the cenozoic cooling: a study based on diversity of plant functional types. Palaios 28 (7), 418–432. https://doi.org/10.2110/palo.2012.p12-096r.
Prentice, I.C., Webb III, T., 1986. Pollen percentages, tree abundances and the Fagerlind effect. J. Quat. Sci. 1 (1), 35–43. https://doi.org/10.1002/jqs.3390010105.
Pringle, R.M., Abraham, J.O., Anderson, T.M., Coverdale, T.C., Davies, A.B., Dutton, C.L., Gaylard, A., Goheen, J.R., Holdo, R.M., Hutchinson, M.C., Kimuyu, D.M., Long, R.A., Subalusky, A.L., Veldhuis, M.P., 2023. Impacts of large herbivores on terrestrial ecosystems. Curr. Biol. 33 (11), R584–R610. https://doi.org/10.1016/j.cub.2023.04.024.
Quiquet, A., Roche, D.M., Dumas, C., Paillard, D., 2018. Online dynamical downscaling of temperature and precipitation within the iLOVECLIM model (version 1.1). Geosci. Model Dev. (GMD) 11 (1), 453–466. https://doi.org/10.5194/gmd-11-453-2018.
R Core Team, 2020. R: A Language and Environment for Statistical Computing. R Foundation for Statistical Computing. https://www.R-project.org/.
Reynolds, R.G., Whallon, R., Ali, M.Z., Zadegan, B.M., 2006. Agent-based modeling of early cultural evolution. In: 2006 IEEE Congress on Evolutionary Computation, vol. 2006. CEC, pp. 1135–1142. https://doi.org/10.1109/cec.2006.1688437.
Riris, P., 2018. Assessing the impact and legacy of swidden farming in neotropical interfluvial environments through exploratory modelling of post-contact Piaroa land use (Upper Orinoco, Venezuela). Holocene 28 (6), 945–954. https://doi.org/10.1177/0959683617752857.
Robson, A.S., Trimble, M.J., Purdon, A., Young-Overton, K.D., Pimm, S.L., Van Aarde, R. J., 2017. Savanna elephant numbers are only a quarter of their expected values. PLoS One 12 (4), 1–14. https://doi.org/10.1371/journal.pone.0175942.
Roche, D.M., 2013. $\delta^{18}O$ water isotope in the iLOVECLIM model (version 1.0) - Part 1: implementation and verification. Geosci. Model Dev. (GMD) 6 (5), 1481–1491. https://doi.org/10.5194/gmd-6-1481-2013.
Roebroeks, W., Villa, P., 2011. On the earliest evidence for habitual use of fire in Europe. Proc. Natl. Acad. Sci. USA 108 (13), 5209–5214. https://doi.org/10.1073/pnas.1018116108.
Roebroeks, W., MacDonald, K., Scherjon, F., Bakels, C., Kindler, L., Nikulina, A., Pop, E., Gaudzinski-Windheuser, S., 2021. Landscape modification by last interglacial neanderthals. Sci. Adv. 7 (51), 1–14. https://doi.org/10.1126/sciadv.abj5567.
Rogers, J.D., Nichols, T., Emmerich, T., Latek, M., Cioffi-Revilla, C., 2012. Modeling scale and variability in human-environmental interactions in Inner Asia. Ecol. Model. 241, 5–14. https://doi.org/10.1016/j.ecolmodel.2011.11.025.

Romanowska, I., Wren, D.C., Crabtree, A., S, 2021. Agent-based modeling for archaeology. In: Agent-Based Modeling for Archaeology. Simulating the Complexity of Societies. The Santa FE Institute Press. https://doi.org/10.37911/9781947864382.

Rowley-Conwy, P.A., Layton, R., 2011. Foraging and farming as niche construction: stable and unstable adaptations. Philos. Trans. R. Soc. Lond. B Biol. Sci. 366, 262–849. https://doi.org/10.1098/rstb.2010.0307.

Salecker, J., Sciaini, M., Meyer, K.M., Wiegand, K., 2019. The nlrx r package: a next-generation framework for reproducible NetLogo model analyses. Methods Ecol. Evol. 10 (11), 1854–1863. https://doi.org/10.1111/2041-210X.13286.

Saltelli, A., Tarantola, S., Campolongo, F., Ratto, M., 2004. Sensitivity Analysis in Practice: a Guide to Assessing Scientific Models. John Wiley & Sons.

Santos, J.I., Pereda, M., Zurro, D., Álvarez, M., Caro, J., Galán, J.M., Godino, I.B.I., 2015. Effect of resource spatial correlation and hunter-Fisher-gatherer mobility on social cooperation in tierra del fuego. PLoS One 10 (4), 1–29. https://doi.org/10.1371/journal.pone.0121888.

Saqalli, M., Salavert, A., Bréhard, S., Bendrey, R., Vigne, J.D., Tresset, A., 2014. Revisiting and modelling the woodland farming system of the early Neolithic Linear Pottery Culture (LBK), 5600-4900 B.C. Veg. Hist. Archaeobotany 23 (S1), 37–50. https://doi.org/10.1007/s00334-014-0436-4.

Scherjon, F., 2019. Virtual Neanderthals: a Study in Agent-Based Modelling Late Pleistocene Hominins in Western Europe. Leiden University, The Netherlands. Published by Global Academic Press, Vianen. ISBN: 9789463803441.

Scherjon, F., Bakels, C., MacDonald, K., Roebroeks, W., 2015. Burning the land: an ethnographic study of off-site fire use by current and historically documented foragers and implications for the interpretation of past fire practices in the landscape. Curr. Anthropol. 56 (3), 299–326. https://doi.org/10.1086/681561.

Serge, M.A., Mazier, F., Fyfe, R., Gaillard, M.J., Klein, T., Lagnoux, A., Galop, D., Githumbi, E., Mindrescu, M., Nielsen, A.B., Trondman, A.K., Poska, A., Sugita, S., Woodbridge, J., Abel-Schaad, D., Åkesson, C., Alenius, T., Ammann, B., Andersen, S. T., et al., 2023. Testing the effect of relative pollen productivity on the REVEALS model: a validated reconstruction of europe-wide Holocene vegetation. Land 12 (5). https://doi.org/10.3390/land12050986.

Sevink, J., Wallinga, J., Reimann, T., van Geel, B., Brinkkemper, O., Jansen, B., Romar, M., Bakels, C.C., 2023. A multi-staged drift sand geo-archive from The Netherlands: new evidence for the impact of prehistoric land use on the geomorphic stability, soils, and vegetation of aeolian sand landscapes. Catena 224. https://doi.org/10.1016/j.catena.2023.106969.

Smith, D.B., 2011. General patterns of niche construction and the management of 'wild' plant and animal resources by small-scale pre-industrial societies. Philos. Trans. R. Soc. Lond. B Biol. Sci. 366, 836–848. https://doi.org/10.1098/rstb.2010.0253.

Snitker, G., 2018. Identifying natural and anthropogenic drivers of prehistoric fire regimes through simulated charcoal records. J. Archaeol. Sci. 95, 1–15. https://doi.org/10.1016/j.jas.2018.04.009.

Sommer, R.S., 2020. Late Pleistocene and Holocene history of mammals in Europe. In: Hackländer, K., Zachos, F.E. (Eds.), Mammals – of Europe – Past, Present, and Future. Springer, pp. 83–98.

Sorensen, A.C., Claud, E., Soressi, M., 2018. Neandertal fire-making technology inferred from microwear analysis. Sci. Rep. 8 (1), 1–16. https://doi.org/10.1038/s41598-018-28342-9.

Stuart, A., Ord, J.K., 1994. Kendall's Advanced Theory of Statistics, Distribution Theory. John Wiley & Sons.

Sugita, S., 2007. Theory of quantitative reconstruction of vegetation I: pollen from large sites REVEALS regional vegetation composition. Holocene 17 (2), 229–241. https://doi.org/10.1177/0959683607075837.

Summerhayes, G.R., Leavesley, M., Fairbairn, A., Mandui, H., Field, J., Ford, A., Fullagar, R., 2010. Human adaptation and plant use in Highland New Guinea 49,000 to 44,000 years ago. Science 330 (6000), 78–81. https://doi.org/10.1126/science.1193130.

Sweeney, L., Harrison, S.P., Linden, M. Vander, 2022. Assessing anthropogenic influence on fire history during the Holocene in the Iberian Peninsula. Quat. Sci. Rev. 287, 107562 https://doi.org/10.1016/j.quascirev.2022.107562.

Tallavaara, M., Luoto, M., Korhonen, N., Järvinen, H., Seppä, H., 2015. Human population dynamics in Europe over the last glacial maximum. Proc. Natl. Acad. Sci. U.S.A. 112 (27), 8232–8237. https://doi.org/10.1073/pnas.1503784112.

Tasser, E., Ruffini, F.V., Tappeiner, U., 2009. An integrative approach for analysing landscape dynamics in diverse cultivated and natural mountain areas. Landsc. Ecol. 24 (5), 611–628. https://doi.org/10.1007/s10980-009-9337-9.

Thompson, J.C., Wright, D.K., Ivory, S.J., Choi, J.H., Nightingale, S., Mackay, A., Schilt, F., Otárola-Castillo, E., Mercader, J., Forman, S.L., Pietsch, T., Cohen, A.S., Arrowsmith, J.R., Welling, M., Davis, J., Schiery, B., Kaliba, P., Malijani, O., Blome, M.W., et al., 2021. Early human impacts and ecosystem reorganization in southern-central Africa. Sci. Adv. 7 (19) https://doi.org/10.1126/sciadv.abf9776.

Trondman, A.-K., Gaillard, M.-J., Mazier, F., Sugita, S., Fyfe, R., Nielsen, A.B., Twiddle, C., Barratt, P., Birks, H.J., Bjune, A.E., Björkman, L., Broström, A., Caseldine, C., David, R., Dodson, J., Dörfler, W., Fischer, E., Geel, B. van, Giesecke, T., et al., 2015. Pollen-based quantitative reconstructions of Holocene regional vegetation cover (plant-functional types and land-cover types) in Europe suitable for climate modelling. Global Change Biol. 21, 676–697. https://doi.org/10.1111/gcb.12737.

Trondman, A.K., Gaillard, M.J., Sugita, S., Björkman, L., Greisman, A., Hultberg, T., Lagerås, P., Lindbladh, M., Mazier, F., 2016. Are pollen records from small sites appropriate for REVEALS model-based quantitative reconstructions of past regional vegetation? An empirical test in southern Sweden. Veg. Hist. Archaeobotany 25 (2), 131–151. https://doi.org/10.1007/s00334-015-0536-9.

U.S. Geological Survey. (n.d.). GTOPO30. https://www.usgs.gov/.

Vannière, B., Colombaroli, D., Chapron, E., Leroux, A., Tinner, W., Magny, M., 2008. Climate versus human-driven fire regimes in Mediterranean landscapes: the Holocene record of Lago dell'Accesa (Tuscany, Italy). Quat. Sci. Rev. 27 (11–12), 1181–1196. https://doi.org/10.1016/j.quascirev.2008.02.011.

Verhagen, P., de Kleijn, M., Joyce, J., 2021. Different models, different outcomes? A comparison of approaches to land use modeling in the Dutch limes. Heritage 4 (3), 2081–2104. https://doi.org/10.3390/HERITAGE4030118.

Vidal-Cordasco, M., Nuevo-López, A., 2021. Resilience and vulnerability to climate change in the Greek Dark Ages. J. Anthropol. Archaeol. 61 https://doi.org/10.1016/j.jaa.2020.101239.

Vrac, M., 2018. Multivariate bias adjustment of high-dimensional climate simulations: the Rank Resampling for Distributions and Dependences (R2D2) bias correction. Hydrol. Earth Syst. Sci. 22 (6), 3175–3196. https://doi.org/10.5194/hess-22-3175-2018.

Warnant, P., Francois, L., Strivay, D., 1994. CARAIB: a global model of terrestrial biological productivity. Global Biogeochem. Cycles 8 (3), 255–270.

Whelan, R.J., 1995. The Ecology of Fire. Cambridge University Press.

Wickham, H., 2016. ggplot2: Elegant Graphics for Data Analysis. https://ggplot2.tidyverse.org.

Wickham, H., Averick, M., Bryan, J., Chang, W., McGowan, L., François, R., Grolemund, G., Hayes, A., Henry, L., Hester, J., Kuhn, M., Pedersen, T., Miller, E., Bache, S., Müller, K., Ooms, J., Robinson, D., Seidel, D., Spinu, V., et al., 2019. Welcome to the tidyverse. J. Open Source Softw. 4 (43), 1686. https://doi.org/10.21105/joss.01686.

Wilensky, U., 1999. NetLogo. http://ccl.northwestern.edu/netlogo/.

Woldring, H., Schepers, M., Mendelts, J., Fens, R., 2012. Camping and foraging in Boreal hazel woodland – the environmental impact of Mesolithic huntergatherers near Groningen, The Netherlands. In: Terberger, M.J.L.T.N., Barton, R.N.E., Street, M. (Eds.), A Mind Set on Flint. Studies in Honour of Dick Stapert. Barkhuis Publishing, pp. 381–392.

Wren, C.D., Burke, A., 2019. Habitat suitability and the genetic structure of human populations during the last glacial maximum (LGM) in western Europe. PLoS One 14 (6), 1–22. https://doi.org/10.1371/journal.pone.0217996.

Zapolska, A., Serge, M.A., Mazier, F., Quiquet, A., Renssen, H., Vrac, M., Fyfe, R., Roche, D.M., 2023a. More than agriculture: analysing time-cumulative human impact on European land-cover of second half of the Holocene. Quat. Sci. Rev. 314 https://doi.org/10.1016/j.quascirev.2023.108227.

Zapolska, A., Vrac, M., Quiquet, A., Extier, T., Arthur, F., 2023b. Improving biome and climate modelling for a set of past climate conditions: evaluating bias correction using the CDF-t approach Improving biome and climate modelling for a set of past climate conditions : evaluating bias correction using the CDF-t approach. Environ. Res. Clim. 2 (2) https://doi.org/10.1088/2752-5295/accbe2.

Zolnikov, I.D., Postnov, A.V., Lyamina, V.A., Slavinski, V.S., Chupina, D.A., 2013. Geoinformation modeling of environments favorable for prehistoric humans of the Altai Mountains. Archaeol. Ethnol. Anthropol. Eurasia 41 (3), 40–47. https://doi.org/10.1016/j.aeae.2014.03.006.

Zvelebil, M., 1994. Plant use in the Mesolithic and its role in the transition to farming. Proc. Prehist. Soc. 60, 35–74.

Zwolinski, M.J., 1990. Fire effects on vegetation and succession. In: Krammes, J. (Ed.), Effects of Fire Management of Southwestern Natural Resources, pp. 18–24. *General Technical Report RM-GTR-191*.